nature mental health

Article

https://doi.org/10.1038/s44220-025-00519-y

Projecting the morbidity burden of mental and behavioral disorders associated with increasing humid heat in Shanghai

Received: 12 September 2024

Accepted: 17 September 2025

Published online: 02 December 2025

Check for updates

Chen Liang[1,2,3], Jiacan Yuan[1,2,4] ✉, Renhe Zhang[1,2,5,47], Xu Tang[1,2,47], Gunter Schumann[6,7,8,9,47] & the environMENTAL Consortium*

Residents of low-latitude megacities face growing vulnerability to humid-heat stress under urbanization and global warming, yet limited research has assessed the morbidity burden of mental and behavioral disorders (MBDs) linked to humid-heat exposures in these cities. Here we quantify the hospital admissions of MBDs in Shanghai, a megacity of over 25 million inhabitants, attributable to humid heat, and project future burdens under various greenhouse gas (GHG)-emission and population scenarios. Humid heat drives a higher morbidity burden than high temperature alone, especially in humid-heat nights. Without population change, the humid-heat-related morbidity burden of MBDs would increase by 68.2% (95% empirical confidence interval 56.7%–81.6%) under the highest-GHG-emission scenario by the 2090s, while 8,465 (95% empirical confidence interval 6,928–10,053) cases would be avoided by reducing emissions to the lowest pathway. With projected population decline, the attributable hospital admissions will decrease toward century's end. These findings highlight the benefit of GHG mitigation in reducing the growing MBD risks posed by extreme humid heat.

Climate change stands out as one of the paramount public health challenges of the twenty-first century[1–5]. With each increment of global warming, regional climate changes and extremes become increasingly prevalent and pronounced. As reported by the Intergovernmental Panel on Climate Change, elevated temperatures are linked with mental-health challenges[6], including increased incidence of psychiatric disorders[7–9], heightened stress levels[10] and greater numbers of suicides[11,12]. Extreme heat events, specifically, are acknowledged to exacerbate underlying mental and behavioral disorders (MBDs), thereby amplifying the rates of mortality and morbidity among individuals with such conditions[13]. The burden of MBDs continues to escalate in the context of global warming, profoundly affecting health outcomes and generating substantial social, human rights and economic ramifications worldwide[14].

Although the relationship between heat exposure and mental health has been documented in recent studies[7–9,15], current assessments

[1]Department of Atmospheric and Oceanic Sciences & Institute of Atmospheric Sciences & Shanghai Key Laboratory of Ocean–Land–Atmosphere Boundary Dynamics and Climate Change, Fudan University, Shanghai, China. [2]IRDR International Center of Excellence on Risk Interconnectivity and Governance on Weather/Climate Extremes Impact and Public Health, Fudan University, Shanghai, China. [3]Shanghai Meteorological Service Center, Shanghai Meteorological Service, Shanghai, China. [4]Shanghai Frontiers Science Center of Atmosphere–Ocean Interaction, Shanghai, China. [5]Key Laboratory of Polar Atmosphere–Ocean–Ice System for Weather and Climate, Ministry of Education, Shanghai, China. [6]Centre for Population Neuroscience and Stratified Medicine, Institute of Science and Technology for Brain-Inspired Intelligence and National Centre for Neurological Disorders, Huashan Hospital, Fudan University, Shanghai, China. [7]Centre for Population Neuroscience and Stratified Medicine (PONS), Charite Mental Health, Department of Psychiatry and Neurosciences, CCM, Charite Universitätsmedizin Berlin, Berlin, Germany. [8]Department of Psychiatry, University of Cambridge, Cambridge, UK. [9]German Center for Mental Health, Berlin, Germany. [47]These authors contributed equally: Renhe Zhang, Xu Tang, Gunter Schumann. *A list of authors and their affiliations appears at the end of the paper. ✉e-mail: jcyuan@fudan.edu.cn

Table 1 | Descriptive environmental statistics of daily hospital admissions for MBDs in the warm season (May to September) in Shanghai

Variable	Mean	Minimum	P_{25}	P_{50}	P_{75}	Maximum
Daily hospital admissions	Mean (total)					
MBDs	37 (17,107)	1	16	36	48	244
Weather conditions	Mean±s.d.					
RH (%)	81.3±8.3	45.8	76.4	82.6	87.3	97.7
Pressure (hPa)	1,007.4±4.4	987.6	1,004.4	1,007.1	1,010.1	1,021.4
Dew point (°C)	21.2±3.7	3.9	18.8	21.8	24.4	27.0
Duration of sunshine (h)	5.0±4.0	0.0	0.8	4.8	8.6	12.5
Temperature (°C)	Mean±s.d.					
Maximum	26.9±3.8	17.7	24.1	26.7	29.2	36.5
Mean	24.8±3.6	15.7	22.5	24.7	27.0	33.2
Minimum	22.9±3.6	12.3	20.7	23.0	25.4	30.4
WBGT (°C)	Mean±s.d.					
Maximum	24.1±3.4	13.0	21.9	24.0	26.8	30.1
Mean	22.9±3.5	11.6	20.8	22.9	25.7	29.0
Minimum	21.7±3.6	10.0	19.6	21.8	24.6	28.0

Abbreviations: P_{25}, 25th percentile; P_{50}, 50th percentile; P_{75}, 75th percentile; RH, relative humidity.

of heat-related morbidity of MBDs have often utilized incomplete measures of heat exposure, typically focusing solely on temperature while neglecting the important role of humidity. Humidity can exacerbate the physiological and psychological stress associated with high temperatures[16–18], thus potentially amplifying mental health issues[4,19,20]. When combined with elevated air temperature, high humidity can reduce the efficiency of evaporative cooling, thereby undermining this cooling mechanism and posing a serious threat to the human body[17]. Adaptation strategies may be less achievable for those with mental illness and thus the affected individuals may be unable to effectively protect themselves from the combined impacts of extreme heat and humidity[21,22]. This oversight is particularly concerning in low- and middle-income countries, where approximately 82% of global mental-health morbidity occurs[23]. In these regions, the combined effects of high temperature and humidity are likely to be more pronounced, yet they are inadequately addressed in current research and climate models.

Of the 4.5 billion people living in urban areas globally about 40–50% live in cities with a hot and humid environment. Although previous research has employed apparent temperature as the indicator of heat[24–27], it was primarily focused on drier climate regions. Urban climates in dry and humid environments are very different, which can lead to differences in urban heat/cold-island effects or wet/dry-island effects[28,29], with corresponding differences in health impacts. This study focuses on the megacity of Shanghai, with over 25 million inhabitants, which is characterized by a very hot and humid summer (Extended Data Fig. 1). Individuals living in such megacities are exposed to many environmental factors that may combine and interact to affect mental health. For instance, urban residents potentially suffer from higher-density residential and commercial buildings, concomitant reduced access to green areas and more stressful social conditions. Given the high personal, public health and economic burden, the need to reduce the prevalence of mental-health problems is a public health priority.

The wet-bulb globe temperature (WBGT) is used in this study to measure the humid-heat exposure, as it provides a more objective reflection of human thermal sensation than temperature itself[30], especially in hot environments[31]. Among the numerous heat-stress indices that have considered humidity, WBGT is an internationally acknowledged humid-heat indicator following the international standard ISO 7243[32]. Additionally, the wet-bulb temperature component of this WBGT index has been refined to more accurately represent the physical process by which high humidity suppresses evaporation[31].

As global warming intensifies, its potential effects on mental health could become a massive and pervasive public-health problem. Projections of how mental-health outcomes may evolve in response to a warming climate are urgently needed. However, the future morbidity burden associated with extreme humid heat under different greenhouse gas (GHG) emission scenarios is currently unknown. Here, we assess the combined effects of temperature and humidity on mental health. By integrating advanced climate models, we project the future impact of climate change on mental health under various GHG-emission and population-change scenarios. Our goal is to provide comprehensive insights that can inform public health policies and interventions, ultimately contributing to the development of adaptive public health strategies and effective mitigation plans.

Results

Descriptive data

A total of 17,107 cases of MBDs were recorded in Shanghai during the warm season (May to September) from 2013 to 2015 (Table 1). Daily hospital admissions averaged 37 cases, peaking at 244 cases per day. The seasonal pattern of the observed daily hospital admissions during the study period is presented in Extended Data Fig. 2. The warm season in Shanghai is hot and humid, with an overall average temperature of 24.8 °C (s.d. = 3.6 °C) and average relative humidity of 81.3% (s.d. = 8.3 °C). The mean WBGT in the warm season over the whole study period was 22.9 °C (s.d. = 3.5 °C). The temporal evolution trends of the above meteorological variables between the warm seasons of 2013 and 2015 can be found in Extended Data Fig. 2c. Meanwhile, the maximum of daily minimum WBGT approached 28 °C, above which only light activities (for example, walking) can be sustained without heat-stroke risk[31]. The daily maximum WBGT could reach 30.1 °C, beyond which physical activities should be halted to maintain a normal core body temperature[32].

Exposure–lag–response relationships of hospital admissions for MBDs

To quantify the linkages between diverse heat metrics and mental health, we estimated the exposure–lag–response relationship of daily mean temperature (T_{mean} hereafter), daily mean WBGT ($WBGT_{mean}$

https://doi.org/10.1038/s44220-025-00519-y

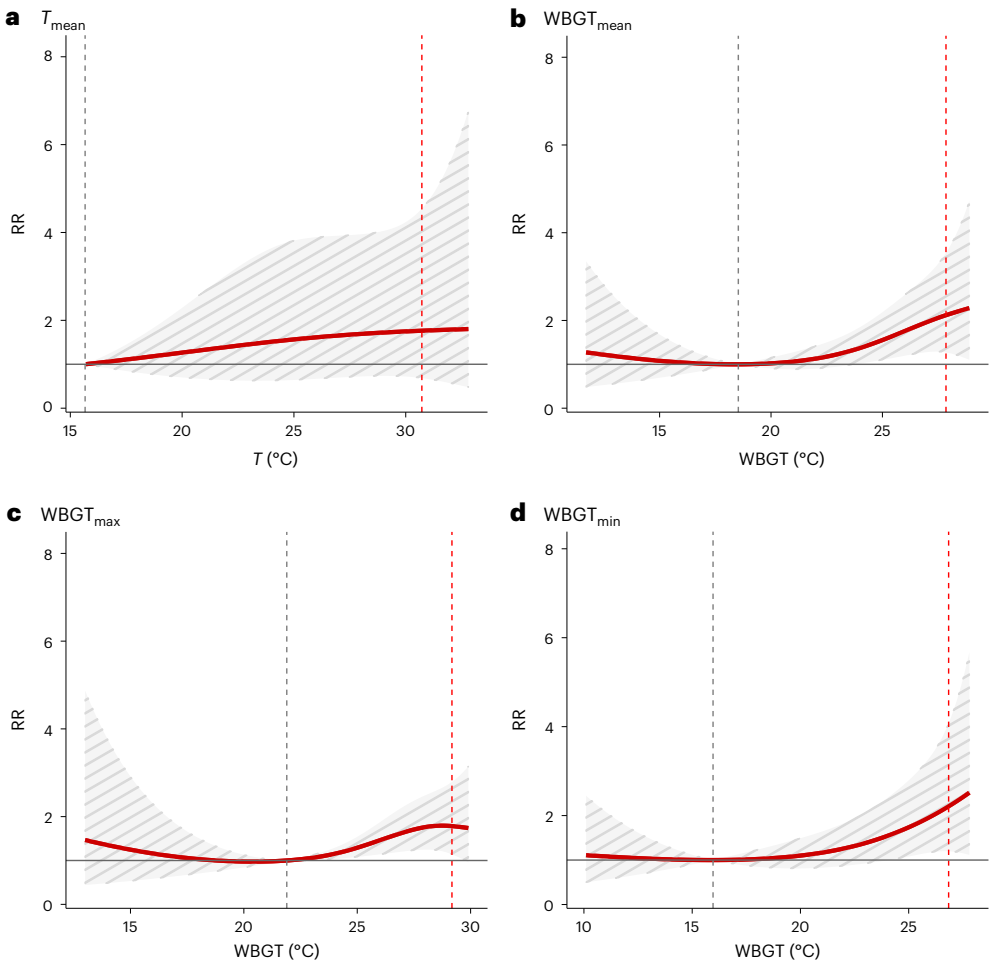

Fig. 1 | Curves for the association between different heat metrics and MBDs hospital admissions in Shanghai. a, Daily mean temperature; **b**, daily mean WBGT; **c**, daily maximum WBGT; **d**, daily minimum WBGT. Solid red lines indicate the estimated RRs and shaded gray areas report the 95% CIs, and the vertical red dotted lines represent the 95th percentile of warm-season temperatures or WBGTs. The vertical gray dotted line represents the minimum morbidity temperature or WBGT (MMT). The gray horizontal line represents RR = 1.

hereafter), daily minimum WBGT ($WBGT_{min}$ hereafter) and daily maximum WBGT ($WBGT_{max}$ hereafter) with MBD hospital admissions at a maximum lag of up to 5 d. The exposure–response relationship of MBD hospital admissions corresponding to different heat metrics displays various features (Fig. 1). The response curves for WBGT metrics (that is $WBGT_{mean}$, $WBGT_{min}$ and $WBGT_{max}$) showed slight 'J' shapes, while the curve for T_{mean} was nearly linear. These curves were represented as relative risk (RR), indicating the increase in morbidity risk associated with specific temperatures compared with a reference value. The reference temperature, set at the level associated with the minimal MBDs risk, is defined as the optimal temperature with an RR of 1. Given the delayed effect caused by heat and humidity, we also examined the lag patterns between daily MBD hospital admissions and the above heat metrics for different lag days among selected cutoff points (Supplementary Table 1). Among the four metrics, the lagged correlation is more pronounced with $WBGT_{mean}$ and $WBGT_{min}$. For a single lag day (for example lag 0, lag 1, …, lag 5), the most positive and statistically significant associations related to extremely high $WBGT_{mean}$ and $WBGT_{min}$ were observed on the concurrent day (lag 0) and the maximum lag day (lag 5), while the RR associated with T_{mean} was less significant. For cumulative lag days (for example cumulating RR from lag 0–1 to lag 0–5), the RRs related to the WBGT metrics at extreme heat level (95th percentile) were statistically significant for both lag 0–1 and lag 0–5, while that associated with T_{mean} was still less significant. These lag patterns demonstrated that humid-heat weather will have a more lasting impact on the incidence of MBDs than high-temperature weather alone.

Moreover, it is evident that $WBGT_{min}$ shows a higher RR in the high-temperature range compared with the other three metrics. The estimated RR at the 95th percentile of $WBGT_{min}$ was 2.23 (95% confidence interval (CI) 1.20–4.14), distinctly surpassing that of T_{mean} (1.76, 95% CI 0.69–4.53), $WBGT_{mean}$ (2.13, 95% CI 1.27–3.58) and $WBGT_{max}$ (1.79, 95% CI 1.16–2.76). Considering that $WBGT_{min}$ typically occurs during the night, these results indicate that days with hot nights hold an elevated morbidity risk for MBDs as compared with days with hot days only.

Projected trends of WBGT

To investigate the effects of future warming on mental health, we projected the change of T_{mean}, $WBGT_{mean}$, $WBGT_{min}$ and $WBGT_{max}$ in Shanghai under four GHG-emission scenarios until the end of this century (Fig. 2). A greater escalation of the projected temperatures and WBGT values is observed under higher-GHG-emission scenarios (for example, Shared Socioeconomic Pathways (SSP) 5-8.5 scenario) throughout the twenty-first century. The temperature is consistently expected to remain higher than the WBGT values. Under medium-GHG-emission scenarios (for example, SSP2-4.5), both temperature and WBGT exhibit stabilizing trends in the latter part of the century. In contrast, under low-GHG-emission scenarios (for example, SSP1-2.6), WBGT is projected to peak in the 2060s, followed by a gradual decline. The warm-season $WBGT_{mean}$ is projected to reach 24.2 °C, 25.1 °C, 26.1 °C and 27.1 °C in the

https://doi.org/10.1038/s44220-025-00519-y

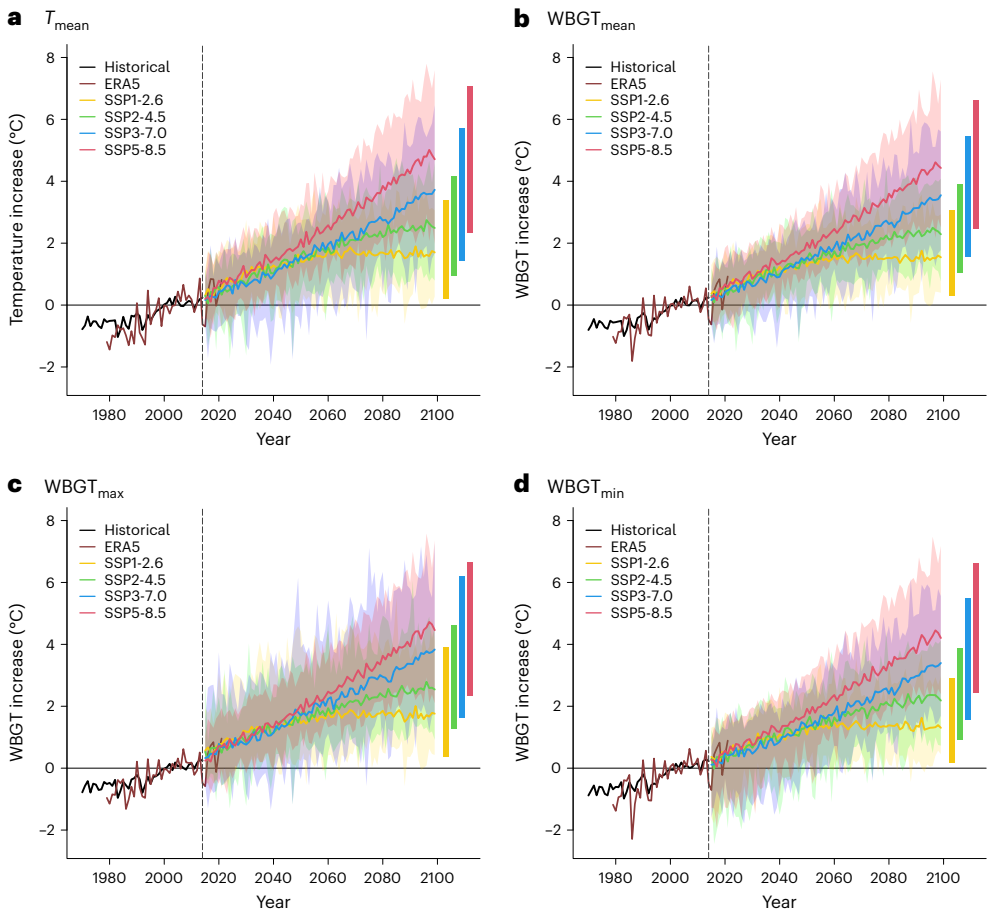

Fig. 2 | Projected increases in different heat metrics under the SSP1-2.6, SSP2-4.5, SSP3-7.0 and SSP5-8.5 scenarios in Shanghai. a, Daily mean temperature; **b**, daily mean WBGT; **c**, daily maximum WBGT; **d**, daily minimum WBGT. All changes were calculated as deviations from the period of 1995–2014 during the warm season. Annual mean series across 19 global climate models (GCMs) for historical, SSP1-2.6, SSP2-4.5, SSP3-7.0 and SSP5-8.5 scenarios are presented in black, yellow, green, blue and red, respectively. Shading indicates the variability, corresponding to the range for each year. The horizontal bars on the right correspond to the average annual maximum and minimum for each projected series. The solid brown line denotes the annual change calculated using European Centre for Medium-Range Weather Forecasts Reanalysis Fifth Generation (ERA5) data from 1979 to 2021, as a comparison with model simulations.

2090s, with increments of 1.3 °C, 2.1 °C, 3.2 °C and 4.1 °C compared with the 2010s under the SSP1-2.6, SSP2-4.5, SSP3-7.0 and SSP5-8.5 scenarios, respectively (Supplementary Table 2).

Projected morbidity burden of MBDs

On the basis of the relationships above, we projected the heat-related attributable fraction (AF) under four GHG-emission scenarios. The AF is widely used to quantify the projected health impact, and is defined as the ratio between excess hospital admissions and the total MBDs hospital admissions (for details see Methods). The AFs of MBDs hospital admissions measured by different heat metrics (T_{mean}, $WBGT_{mean}$, $WBGT_{max}$ and $WBGT_{min}$) are expected to undergo a substantial increase in the context of future warming, especially for $WBGT_{mean}$ and $WBGT_{min}$ (Fig. 3). Under the SSP1-2.6 scenario, the AF experiences gradual growth first and then stabilizes after the 2060s. In contrast, under the other three scenarios, the AF is projected to steadily increase throughout the century, with more pronounced trends evident under higher-emission scenarios. Under the SSP5-8.5 scenario, the AF due to $WBGT_{mean}$ could achieve 68.2% (95% empirical confidence interval (eCI) 56.7%–81.6%) by the 2090s. Furthermore, the increase of AF associated with $WBGT_{mean}$ is approximately 6% higher than that related to T_{mean}. This indicates a significant increase in the future morbidity risk attributable to the humid-heat weather conditions. Among the three WBGT metrics, $WBGT_{max}$ shows the lowest morbidity burden and the least pronounced upward trend. We hypothesized that this may be due to $WBGT_{max}$ typically occurring in the afternoon, a time when individuals are more likely to adopt protective measures, such as reducing outdoor activity or seeking shaded and cooled environments, which may partially mitigate the health risks associated with humid heat. While behavioral adaptations are not explicitly included in the exposure–response function, their effects are implicitly captured through the observed data used for analysis. Additionally, the AF associated with $WBGT_{min}$ attains the highest level, emphasizing the substantial morbidity risk posed by mental illness during humid-heat nights, which should not be overlooked.

To highlight the morbidity risks only brought by climate warming, we estimated the RRs at an extreme heat level (99th percentile of ambient temperature/WBGT) in the 2090s and the heat-related AFs of MBDs hospital admissions in the 2030s, 2060s and 2090s relative to the baseline period (2010–19) (Extended Data Fig. 3). Notably, the RRs at extreme heat increase with the elevation of GHG-emission scenarios. Similarly, we observed an increased morbidity risk attributed to humid-heat nights. Evidence for this can be found in the RR associated with $WBGT_{min}$, which exhibits the highest value (RR 3.13, 95% CI 0.88–11.13) in the 2090s under the SSP5-8.5 scenario, more than twice the RR of T_{mean} (RR 1.82, 95% CI 0.39–8.54) (Extended Data Fig. 3a). Furthermore, whether in the 2030s, 2060s or 2090s, the heat-related AFs from humid-heat weather surpass those from high-temperature weather alone (Extended Data Fig. 3b–d). Specifically, the AF associated with $WBGT_{mean}$ (31.8%, 95% eCI 20.6%–43.2%) is almost three times

https://doi.org/10.1038/s44220-025-00519-y

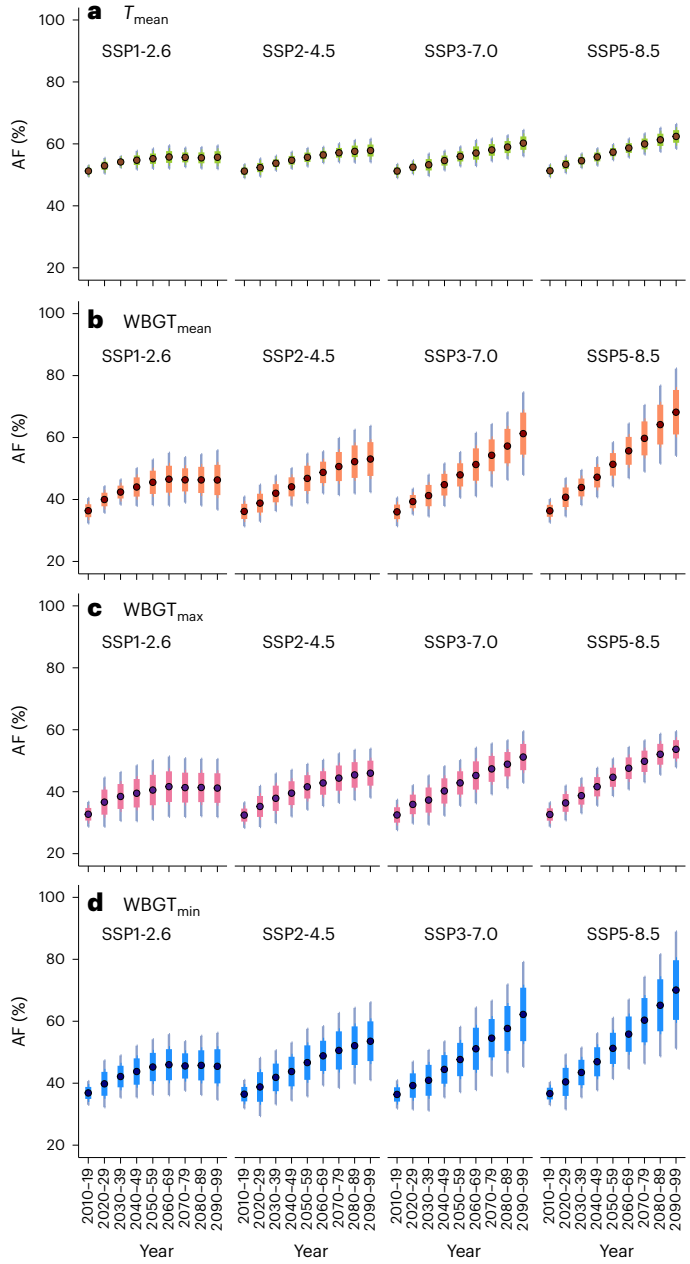

Fig. 3 | Projections of heat-related AFs for MBDs hospital admissions due to the heat metrics under different GHG-emission scenarios in Shanghai. **a**, Daily mean temperature; **b**, daily mean WBGT, **c**, daily maximum WBGT; **d**, daily minimum WBGT. Projections were derived from the ensemble mean of the 19 GCMs. Green, orange, pink and blue colors represent the outcomes associated with T_{mean}, $WBGT_{mean}$, $WBGT_{max}$ and $WBGT_{min}$, respectively. Dots indicate the estimated mean value, with boxes indicating one s.d. Gray vertical lines denote the 95% eCIs.

higher than that related to T_{mean} (11.1%, 95% eCI 7.8%–14.2%) under the SSP5-8.5 scenario by the end of this century. Although the AFs of MBDs are still projected to increase relative to the baseline period even under the scenario with the strictest control of GHG emissions (SSP1-2.6), there is minimal discernible variation in the magnitude of AFs associated with different metrics over time. The findings highlight the importance of reducing GHG emissions for mental health in the context of global climate change.

Assuming that future population size is fixed at the present level, the heat-related attributable number (AN) of MBDs hospital admissions exhibits a consistently increasing trend in the future, closely resembling the trend depicted in Fig. 3 for AFs (Fig. 4). The numbers of attributed hospital admissions initially increase steadily, then stabilize after the 2060s under low-GHG-emission scenarios, while displaying continuously increasing trends under high-GHG-emission scenarios. At the same time, it can be observed that the number of heat-attributable hospital admissions related to $WBGT_{max}$ is the lowest among all heat metrics. The AN related to $WBGT_{mean}$ and $WBGT_{min}$, especially $WBGT_{min}$, demonstrates a more substantial increase than that related to T_{mean}, particularly under high-GHG-emission scenarios such as SSP3-7.0 and SSP5-8.5. Specifically, under the SSP5-8.5 scenario, heat-related AN associated with $WBGT_{min}$ is projected to reach 26,381 (95% eCI 21,591–33,601) cases by the 2090s, exceeding that associated with $WBGT_{mean}$ by 670 cases (95% eCI 291–2,718). If we solely consider the impact of climate change, humid-heat events would impose a greater morbidity burden of MBDs compared with high temperature alone.

According to a recent population projection that considered diverse fertility and migration scenarios[33], Shanghai's population will experience a significant decline in the future no matter what SSP-based scenario is followed (Extended Data Fig. 4). We incorporated the projected population changes in Shanghai into our estimation of heat-related ANs (Fig. 4). Accounting for future population changes, ANs peak mid-century and then gradually decrease. The projected decline of ANs under future scenarios is closely linked to the projected decreases in population of Shanghai, which are mainly driven by persistently low fertility rates, accelerated aging and restricted migration under most SSP-based scenarios[34]. Likewise, the ANs are significantly higher under higher-GHG-emission scenarios than those under low- or medium-GHG-emission scenarios. Notably, the AN related to T_{mean} is higher than that associated with WBGTs before the middle of this century. This suggests that the adverse effects of high temperature, irrespective of high humidity, are also crucial and cannot be overlooked. After the 2060s, humid-heat weather is expected to result in a higher MBDs morbidity burden compared with solely high-temperature conditions, with an increased risk of incidence during humid-heat nights.

The projected number of heat-attributable MBDs hospital admissions was also examined in the 2030s, 2060s and 2090s relative to the baseline period (2010–19) under four GHG-emission scenarios, with and without population changes (Extended Data Fig. 5). When considering population change (Extended Data Fig. 5a–c), the heat-related ANs decrease over time relative to the baseline period, with the most significant decline by the century's end. The largest decrease can be seen in the AN associated with T_{mean}, falling to −11,661 (95% eCI −12,357 to −11,177) cases under the SSP5-8.5 scenario. When assuming no population changes in the future (Extended Data Fig. 5d–f), heat-related ANs gradually increase with the rise of GHG-emission scenarios, particularly those associated with $WBGT_{mean}$ and $WBGT_{min}$. Specifically, by the 2090s, compared with the current climate status (2010–19), the AN related to $WBGT_{mean}$ increases to 12,233 (95% eCI 7,860–16,542) cases under the SSP5-8.5 scenario, which is almost three times that under SSP1-2.6 (3,762, 95% eCI 1,107–7,070). Furthermore, if no action is taken to control GHG emissions, the AN associated with $WBGT_{min}$ is projected to continue rising, gradually surpassing that associated with $WBGT_{mean}$, reaching 12,774 (95% eCI 7,867–19,164) cases under the SSP5-8.5 scenario by the end of this century.

Conclusions and discussion

This study reveals the nonlinear and lagged effects of humid-heat exposure, characterized by WBGT, on MBDs hospital admissions in the Chinese megacity Shanghai, as well as their future risks under various GHG-emission scenarios. Furthermore, we made projections taking into account the effects of changes in population size due to population fertility/migration on mental-health risks. Unlike the previous studies using only one exposure indicator (for example, temperature) to estimate the RR, we derived varying RRs for different indicators such as T_{mean}, $WBGT_{mean}$, $WBGT_{min}$ and $WBGT_{max}$ according

https://doi.org/10.1038/s44220-025-00519-y

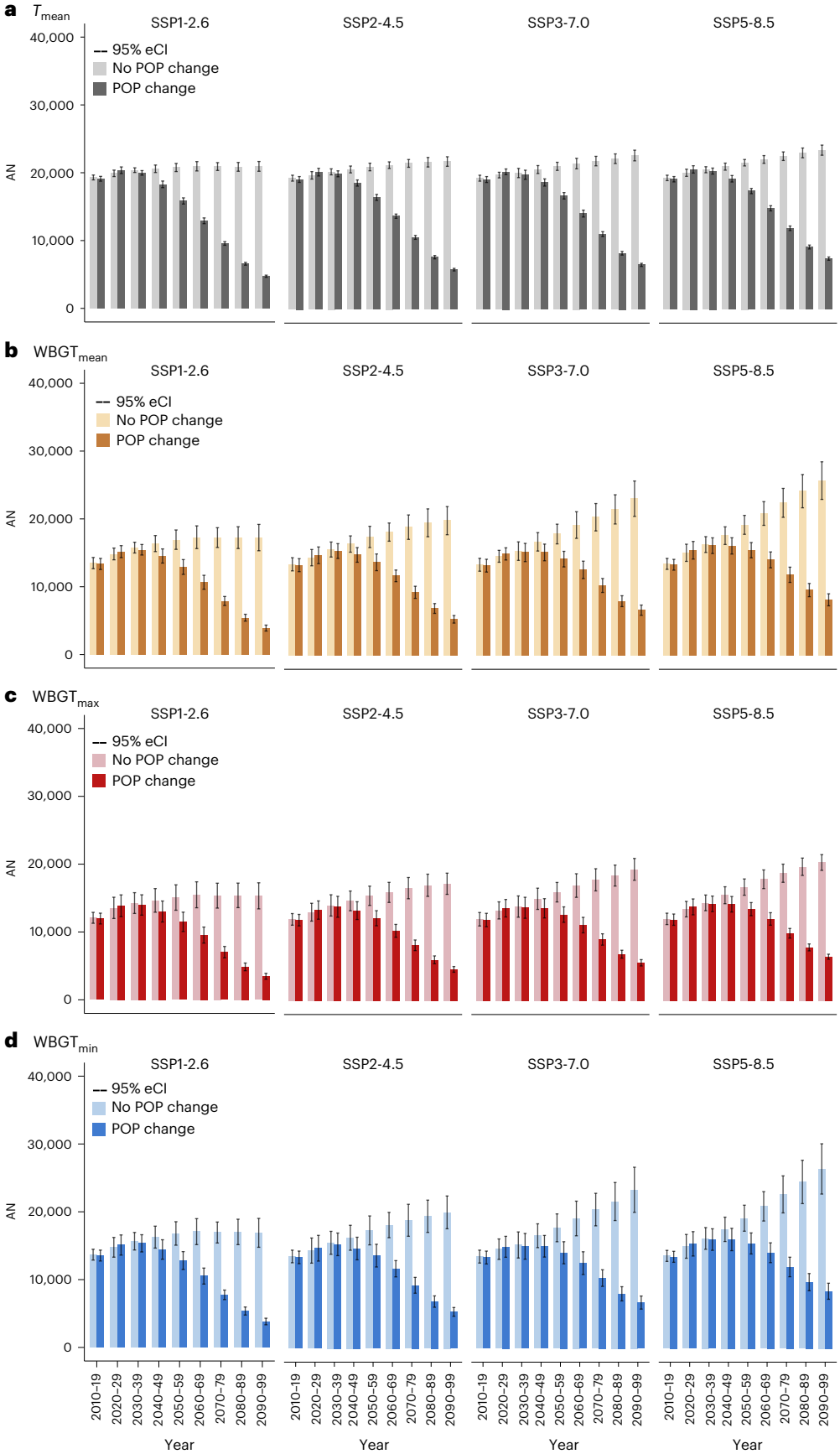

Fig. 4 | Projections of heat-related ANs for MBDs hospital admissions due to the heat metrics under different GHG-emission scenarios. a, Daily mean temperature; **b**, daily mean WBGT; **c**, daily maximum WBGT; **d**, daily minimum WBGT. The gray, yellow, red and blue bars respectively represent the estimated ANs associated with T_{mean}, $WBGT_{mean}$, $WBGT_{max}$ and $WBGT_{min}$, with dark and light colors indicating scenarios with or without population changes. The error bars represent the 95% eCIs based on the simulations by 19 GCMs from Coupled Model Intercomparison Project Phase 6 (CMIP6).

to the specific referent temperatures, which may provide more information for the development of health protection plans to address adverse mental-health risks associated climate warming. By comparing the morbidity burden associated with different heat metrics in various GHG-emission and population-change scenarios, we found that psychiatric patients are more affected by humid-heat extremes than by high temperatures alone, and the morbidity risk at night is higher than that in the daytime. Regardless of whether population changes are considered, humid-heat-related attributable incidence of MBDs would be 113.3–119.3% of current levels (2010–19) in the 2030s due to GHG emissions. Even in the lowest-GHG-emission scenarios (SSP1-2.6), significant increases can be observed in the morbidity risks attributable to high WBGTs, where the RR at an extreme humid-heat level could approach 2.21 (95% CI 1.20–4.06) by the 2090s. Although future population decline will lead to a decrease in ANs, the levels of attributable incidence under SSP5-8.5 are still projected to be higher than those under SSP1-2.6. Mitigating the GHG emissions from the level of SSP5-8.5 to that of SSP1-2.6 could avoid 8,465 (95% eCI 6,928–10,053) humid-heat-related MBDs outpatient visits by the end of this century.

The underlying mechanisms for the association between higher WBGTs and MBDs, albeit as yet not proven, are plausible. Humid heat may exacerbate preexisting mental health problems and lead to mental and behavior disorders through several pathways. A potential etiological mechanism is the disrupted sleep or daytime discomfort during periods of humid-heat extremes[35,36], which may result in hopelessness, maladaptive anxiety, stress and other poor mental health conditions[37–39]. Evidence from time use surveys demonstrated that the warming climate is projected to substantially reduce sleep duration, with particularly pronounced impacts on days characterized by heat waves[40]. Moreover, in high-temperature environments, the human body dissipates heat primarily through excessive sweating, which leads to the loss of water and electrolytes such as sodium, potassium and chloride. Inadequate replenishment of these substances may result in electrolyte imbalances, which can have adverse effects on mental health[41]. For instance, hyponatremia (low sodium levels) may cause confusion, hallucinations, seizures and even coma[42]. Dehydration and electrolyte disturbances have also been associated with increased risks of anxiety, depression and other mood disorders[43]. A recent study revealed that a humid-heat environment can harm mental health and cause anxiety-like behavior by impairing the gut microbiota and related metabolites[44]. Furthermore, patients with preexisting mental disorders are more vulnerable to humid-heat weather conditions than are the general population. Certain medications commonly prescribed for MBDs—such as antipsychotics, antidepressants and mood stabilizers—may impair thermoregulation and further disrupt electrolyte balance[45–47]. Anticholinergic agents, for example, can suppress sweating and thereby increase the risk of heat stroke, while diuretics may promote electrolyte loss and exacerbate dehydration[48]. Moreover, the individual's illness may decrease the ability to remain themselves cognitively aware of the surrounding environment: neglecting appropriate prevention measures such as drinking extra fluids, taking off clothing when required and avoiding going outside[49,50]. These factors collectively increase the vulnerability of individuals with MBDs to heat-related health risks under extreme temperature or humid-heat conditions. Although the presence of air conditioning is protective against temperature-related exacerbation of health conditions, individuals with mental and behavioral illness often have lower socioeconomic status compared with the general population, which could affect their ability to live in an air-conditioned environment[51]. In particular, most low- and middle-income countries give low priority to mental health compared with other burdensome health conditions such as communicable and non-communicable physical diseases.

Some limitations of our study need to be acknowledged. First, this study does not incorporate spatial variations, especially in urban environments, which can generate heterogenetic vulnerability patterns in response to extreme temperatures[52]. Second, our projections of future MBDs morbidity burden are virtually based on the baseline morbidity status, the current socioeconomic conditions and level of vulnerability[53,54]. We assumed that the exposure–response function in the future would remain the same as under current climate conditions. This assumption may introduce biases when assessing future projections of attributable hospital admissions for MBDs. Third, the limited sample size currently available for MBDs hospital admissions has constrained our ability to conduct an in-depth analysis of age and gender. Future work should take into account effects of population aging, urbanization patterns, air pollutants and socioeconomic development on mental-health risks from climate change. Finally, we adopted a simplified WBGT for indoor, shaded outdoor and nighttime conditions because of a lack of necessary radiative variables in climate models from the CMIP archive to calculate future projections of radiative temperature due to sunlight. The simplified WBGT may underestimate WBGT values in daylight hours for locations receiving direct sunlight, but it accurately captures the WBGT for the indoor, shaded outdoor and nighttime conditions (Extended Data Fig. 6). This indicates that the simplified WBGT provides a conservative estimation of heat-related hazards. In addition, the simplified WBGT can serve as an adequate index for assessing the heat risks of MBDs in Shanghai, as most permanent residents experience heat exposure indoors, in shaded outdoor areas or at night.

The present study demonstrates that humid-heat weather poses a notable risk to the well-being of those with MBDs living in megacities, with the risk being even higher at night than during the day. These findings can inform the planning of mitigations and provide potential indicators for adaptations to reduce the risks of climate changes on mental health in the Chinese megacity Shanghai. As compounded heat and humidity extremes are very likely to occur more frequently worldwide[6], our findings may be useful for risk management of mental health in other cities under humid climate regions. Enhancements in the GHG mitigation and humid-heat adaptation strategies must be prioritized to avert substantial economic and social costs associated with humid-heat-related psychiatric morbidity and mortality exacerbated by climate change.

Methods

Study area

Shanghai is located in the Yangtze River Delta in East China, at latitude 30° 40′–31° 53′ N and longitude 120° 52′–122° 12′ E (Extended Data Fig. 1). It is a prominent financial hub in China, which achieved a gross domestic product of 4.72 trillion RMB in 2023, accounting for 3.74% of the total national gross domestic product[55]. Shanghai is one of the most densely populated cities in China, with a permanent population of 24.87 million in 2023[55]. The city has a monsoon-influenced humid subtropical climate with four distinct seasons. Due to the East Asian monsoon, the warm season from May to September is hot and humid. The average annual temperature is approximately 23 °C–28 °C in the summer season. The average annual precipitation is approximately 1,000–1,200 mm, with 60% of the rainfall occurring during May and September. Therefore, Shanghai was chosen to examine humid-heat-related morbidity associations in urban populations.

Data collection

The daily count of hospital admissions was chosen as the outcome metric to represent the acute impact of WBGT on the morbidity of mental illness (Table 1). The records of daily hospital admissions for MBDs from 1 January 2013 to 31 December 2015 were obtained from the electronic archives of Shanghai Health Insurance Bureau (SHIB). SHIB is the government agency in charge of the Shanghai Health Insurance System, which provides compulsory universal health insurance and covers most of the permanent residents in Shanghai (the coverage

rate was 99.6% in 2021). In Shanghai, all hospitals are contracted with the SHIB[56]. Several previous epidemiologic studies have used the SHIB database[7,16]. This work included all registered residents who participated in the Shanghai Health Insurance System. On the basis of the tenth version of the International Classification of Diseases, all hospitalization records of MBDs coded F00–F99 were incorporated into the analysis. Since this study focuses on heat-related morbidity risks of MBDs, only data from the warm season (May to September) are included in the analysis. The study protocol was approved by the institutional review board at the School of Public Health, Fudan University (no. 2021-04-0889). All analyses were conducted at the aggregate level and no participants were contacted.

To explore the climatic characteristics of the Shanghai city, we collected daily meteorological data from Shanghai Meteorological Bureau during the period of 2013–15, including daily average temperature, daily minimum temperature, daily maximum temperature, relative humidity, wind velocity, sunshine duration and barometric pressure. Meanwhile, the hourly meteorological data from the ERA5 reanalysis product were collected to establish the exposure–response function between MBDs and humid-heat weather conditions. Three meteorological variables (that is, 2-m temperature, t2m, 2-m dew-point temperature, d2m, and surface pressure, sp) with 0.25° × 0.25° spatial resolution were collected from the ERA5 dataset to calculate the daily mean, minimum and maximum WBGT indices. In this study, we used temperature and WBGT from ERA5 to identify high-temperature and humid-heat exposure, respectively, as both variables show strong agreement with observational data in Shanghai (Extended Data Fig. 7).

Scenario models

We acquired projected meteorological variable series from 19 GCMs from the latest internationally coordinated CMIP6 during the period of 1970 to 2100 (Supplementary Table 3). Each GCM dataset contains daily WBGT series for historical (1970–2014) and projected (2015–2100) periods. Four different SSP scenarios, SSP1-2.6, SSP2-4.5, SSP3-7.0 and SSP5-8.5, were chosen. Future scenarios represent trajectories of increase in anthropogenic forcing, which is dominated by changes in GHG emissions, and cover the range of possible future development of anthropogenic drivers of climate change found in the literature[57]. They start in 2015 and include scenarios characterized by high and very high GHG emissions (SSP3-7.0 and SSP5-8.5), which project a doubling of CO_2 emissions from current levels by 2100 and 2050, respectively. Additionally, scenarios with intermediate GHG emissions (SSP2-4.5) are considered, wherein CO_2 emissions are projected to remain approximately constant until the mid-century. Furthermore, scenarios featuring low GHG emissions are explored, with CO_2 emissions declining to net zero around or after 2050, followed by diverse levels of net negative CO_2 emission (SSP1-2.6)[58,59]. The modeled daily WBGT series were downscaled through bilinear interpolation at a 0.5° × 0.5° spatial resolution and were all linearly interpolated[53]. We acknowledge that discrepancies may arise when applying the modeled WBGT series to the exposure–response relationships derived from the observed series. To correct the system bias of the model simulations from the observations, we adopted the statistical bias correction method developed by Hempel et al.[60]. In detail, the differences of seasonal cycles between the simulations and observations during the reference period (1995–2014) are corrected from each calendar day of the simulated data. The method adjusts the daily variability of the simulated data to ensure that their seasonal cycle aligns with the observed seasonal cycle, and preserves the long-term trend and variability of the original data[61]. A comparison between the observed and modeled series is illustrated in Extended Data Fig. 8. In general, the modeled series can be reproduced with minor differences between the model and observations. Therefore, we are confident that the selected GCMs are capable of accurately projecting daily WBGTs in the future.

The future population projection dataset used in this study is from ref. 33. The dataset was constructed utilizing data gathered during the Sixth National Population Census, with the reference year set to 2010. By incorporating the influences of multiple factors, including birth, death and migration, Zhang et al. presented a comprehensive set of future population projections at the city, provincial and national levels under 15 different scenarios from 2010 to 2100[33]. This dataset developed a set of five fertility scenarios and three migration scenarios to overcome the limitation associated with the application of SSPs in the context of China, since the commonly used SSPs, particularly inequality SSP4 and fossil-fuel-dominant SSP5, may be less applicable to China due to recent comprehensive poverty-reduction efforts, compulsory education policies and carbon neutrality goals. Given that the focus of this study primarily pertains to Shanghai, where future population changes exhibit minimal variations across three migration scenarios, primarily influenced by fertility scenarios, we therefore assumed a moderate migration scenario (Migr2) for Shanghai and selected five fertility scenarios (Fer1 to Fer5) to estimate the future burden of MBDs. Furthermore, as the population trends in Shanghai under scenarios Fer4 and Fer5 nearly overlap (Extended Data Fig. 4), we ultimately selected the highest-fertility scenario (Fer5) to represent the high-fertility scenario for future estimations. A no-population-change scenario was also considered as a reference group to highlight the impact of climate change on the morbidity burden of MBDs.

Calculation of WBGT

In this work, humid-heat exposure is characterized using the WBGT index, which is widely used as a heat index developed to incorporate the combined effects of temperature and humidity on thermal comfort. It has been adopted as the international standard ISO 7243, which is used worldwide by agencies to assess heat stress on workers in hot environments[62]. The original version of WBGT is defined as[30]

$$\mathrm{WBGT} = 0.7T_{\mathrm{wb}} + 0.1T_{\mathrm{a}} + 0.2T_{\mathrm{g}} \quad (1)$$

where T_a is the near-surface air temperature, T_{wb} is the near surface wet-bulb temperature and T_g is the globe temperature. Since the radiative variables used to calculate T_g in Liljegren's model[63] are not provided in the projections of many climate models in the CMIP6 archive, this prevents generation of future projections of T_g. Therefore, following previous literature[31,32], we adopt the simplified WBGT for indoor or outdoor shaded conditions:

$$\mathrm{WBGT} = 0.7T_{\mathrm{wb}} + 0.3T_{\mathrm{a}} \quad (2)$$

The simplified WBGT, which neglects the effect of direct sunshine, provides a conservative estimate of the heat conditions in Shanghai. While it may underestimate heat-related hazards during daylight hours for locations receiving direct sunlight, it accurately captures heat risks in indoor, shaded outdoor and nighttime conditions. Most permanent residents in Shanghai experience heat exposure in these three conditions. According to estimates from the Shanghai Population Census Yearbook 2020[64], approximately 1.1% of permanent residents are engaged in outdoor work. Shanghai's labor protection regulations for high-temperature conditions require employers to adjust working hours to minimize outdoor work during the hottest periods of the day and to provide cooling facilities to ensure employee health and safety during heat waves. Furthermore, shading structures and cooling shelters are widely implemented in outdoor public spaces and streets across the city. In addition, various sun protection measures, such as umbrellas, UV-protective clothing and wide-brimmed hats, are commonly used by Shanghai residents. These measures effectively reduce direct sunlight exposure during heat waves, further supporting the applicability of simplified WBGT in evaluating heat-related risks in the region.

As a key component of WBGT, T_{wb} herein is calculated as the 'isobaric wet-bulb temperature', which is defined as the temperature an air parcel attains after it is saturated by water evaporated into it, with the whole air–water system kept under constant pressure and insulated from the environment[65]. We calculate the isobaric wet-bulb temperature by solving an enthalpy balance equation between the initiated condition and saturated condition of moist air (ref. 31, Supplementary Information):

$$c_{pa}T_w + L_v r_s(T_w) = c_{pa}T_a + rL_v \quad (3)$$

where c_{pa} is the specific heat capacity of air under constant pressure, L_v is the latent heat of evaporation of water, r is the initial specific humidity and $r_s(T_w) = P_{sat}(T_w)/P$ is the equilibrium specific humidity, dependent on the saturation water vapor pressure at temperature T_w. The T_w obtained by this approach is the isobaric wet-bulb temperature[31]. It more closely resembles the physical mechanisms of humidity influencing a human's cooling efficiency through perspiration compared with another widely used approach, which calculates T_w relevant to pseudo-adiabatic processes in convective systems[66]. To calculate the isobaric wet-bulb temperature, the near-surface air temperature (T_a) and barometric pressure (P) are required, along with a variable for initial water vapor content, such as specific humidity, or dew-point temperature.

Statistical analysis

Association between WBGT and daily hospital admissions for MBDs. To assess the distributed lag effect of WBGT on daily hospital admissions of MBDs, a quasi-Poisson generalized additive model combined with a distributed lag nonlinear model (DLNM) was applied, motivated by previous studies[7,8,25,67]. The DLNM is built on the foundation of combining two functions (exposure and lag) into a 'cross-basis', a bi-dimensional matrix that allows the estimation of possible nonlinear WBGTs and morbidity effects across specific lag periods[68,69]. On the basis of the DLNM model, we can calculate the immediate effect of the event (lag 0), the delayed effect on day N after the event (lag N) and the cumulative effect during the period (lag 0–N)[7]. The model representation to describe the time series of health outcomes (the number of daily hospital admissions) is as follows:

$$\log(E(Y)) = \alpha + \mathrm{cb}(\mathrm{WBGT}_t, \mathrm{lag} = 5) + \mathrm{ns}(\mathrm{time}_t, \mathrm{df} = 7\,\mathrm{yr}^{-1}) + \mathrm{dow}_t + \mathrm{holiday}_t + \mathrm{HW}_t \quad (4)$$

where Y denotes the time series of daily MBDs hospital admissions, $E(Y)$ corresponds to its expected value, α is the intercept and $\mathrm{cb}(\mathrm{WBGT}_t, \mathrm{lag} = 5)$ is the cross-basis matrix of daily mean WBGT on day t with five lag days, produced by the DLNM that combines the exposure–response and lag–response associations. The exposure–response association was modeled with a natural cubic spline, with two internal knots placed at the 50th and 90th percentiles of the daily WBGT distribution in the observational period. The lag–response association was modeled with two internal knots placed at equally spaced intervals in the log scale. The maximum lag day was set to 5 d to investigate the short-term effect of WBGT in hot environments, on the basis of previous studies[70,71]. We also incorporated the following covariates in the model to account for the potential confounding effects: (1) $\mathrm{ns}(\mathrm{time}_t, \mathrm{df} = 7\,\mathrm{yr}^{-1})$, a natural cubic spline with seven degrees of freedom (df) per year to adjust for the seasonal and long-term time trends; (2) dow_t, corresponding to a categorical variable to control for the day of the week; (3) $\mathrm{holiday}_t$, a binary variable indicating whether day t is a public holiday or not (1 or 0); (4) HW_t, classified as a dichotomous variable with 1 for heat-wave days and 0 for non-heat-wave days. In the present study, we defined a heat wave as ≥2 consecutive days with daily mean WBGT at or above the 95th percentile of the year-round distribution in calendar days during the period of 1995–2014[72]. Here, we used the period from 1995 to 2014 as the reference period to determine this threshold for extreme humid heat. HW_t was included in the model as a binary covariate representing extreme humid-heat events, in addition to the continuous WBGT term. It was introduced to capture additional variability associated with episodic extreme heat that may not be fully explained by the continuous WBGT exposure. The final model was chosen on the basis of the quasi-Akaike information criterion. Smaller quasi-Akaike information criterion values refer to the preferred model[73]. Because we were concerned with heat, we included only summer months in our analyses (May–September). For brevity, we use the term 'heat' as a synonym for high temperature and the term 'humid heat' for compound high temperature and high humidity, although we acknowledge that these terms are used in other contexts[74].

In addition, we compared the fitting effect of models employing daily mean temperature, daily maximum WBGT and daily minimum WBGT as independent variable, using the same analytic framework and model parameters. Daily maximum WBGT generally occurred during the day, and daily minimum WBGT occurred during the night. The purpose of these comparative studies is to provide policy-makers and the public with more reference information.

Projection and quantification of the effect on morbidity. Controlling for the aforementioned covariates in the DLNM, we computed the RRs and 95% CIs of the MBDs hospital admissions at the 5th, 50th, 75th and 95th percentiles of warm-season WBGTs/temperatures relative to the MMT for cumulative lag effect from 0 to 5 d, respectively (Supplementary Table 1 and Extended Data Fig. 9). This analysis assessed the impact of hot, humid and hot, extremely hot and extremely humid-heat weather for MBDs hospital admissions. The MMT, regarded as the optimum temperature, was chosen as the WBGT/temperature corresponding to minimum morbidity risk ($\mathrm{RR}_{MMT} = 1$) and determined by using the best linear unbiased prediction of the cumulative exposure–response relationship. At the same time, it was also recognized as the reference to calculate the fractions and the numbers of excess hospital admissions attributable to the non-optimal temperature.

Due to global warming, future distributions of WBGT (or temperature) are projected to shift toward higher values, potentially exceeding the observed range under current climate conditions. This necessitates the extrapolation of exposure–response relationships beyond the boundaries of currently observed thermal extremes. A feasible approach involves log–linear extrapolation based on exposure–response curves to extend predictions beyond the observed boundaries. In this study, we implement an extrapolation framework by replacing quadratic B-spline functions with natural cubic spline functions sharing identical knots for modeling two-dimensional functions. The proposed methodology employs future projected WBGT (or temperature) sequences to estimate the heat-related morbidity risks under different climate change scenarios (Extended Data Fig. 10). This analytical framework is contingent upon two foundational hypotheses: (1) the estimated exposure–response association remains constant within the currently observed range, explicitly excluding potential modifications from population adaptation or temporal variations in baseline mortality/morbidity rates; (2) the extrapolation appropriately represents the RRs in unobserved thermal ranges beyond existing observational data.

Assuming that the risk of MBDs was associated with high WBGT, the humid-heat-related AF was derived from WBGT beyond the MMT. To estimate the AF of MBDs related to WBGT over future periods under different climate and population change scenarios, we first calculated the excess hospital admissions using the cumulative RR obtained from the exposure–response relationship for a given WBGT in the simulated series of each GCM and scenario on each day. The number of hospital admissions attributed to high WBGTs was then aggregated by a defined time interval for a future period. In this study, this time interval was set to one decade. The corresponding AF was computed

as the ratio between excess MBDs hospital admissions and the total MBDs admissions[53,61,75]. The calculation is as follows:

$$\mathrm{AF} = \frac{\mathrm{RR} - 1}{\mathrm{RR}} \times 100 \quad (5)$$

and the number of MBDs hospital admissions attributable to humid heat can be expressed as

$$\mathrm{AN} = Y_b P_{ssp} \mathrm{AF} \quad (6)$$

where Y_b is the city-level baseline morbidity rate, which denotes the daily average rate of MBDs hospital admissions during the period 2013–15 assuming that there are no changes in the rate in the future; P_{ssp} is the projected population in each period in Shanghai according to the SSP-based scenarios. The resultant AF and AN were subsequently aggregated for each decade up to the 2090s. We also calculated the changes and percent changes for the period 2020–99, using the baseline period 2010–19 as reference.

The main source of uncertainty in the AF and AN are related to the estimation of the exposure–response relationships, especially regarding the range over which we extrapolated the curve, and the variability in WBGT projections. To account for both sources of this uncertainty, we conducted 1,000 Monte Carlo samples by resampling from both the spread of projections across the 19 GCMs and the estimated spline model coefficients. The results were reported as point estimates, using the average across climate models (GCM-ensemble) obtained by the estimated coefficients, and as eCIs, defined as the 2.5th and 97.5th percentiles of the empirical distribution across the samples of coefficients and GCMs. These eCIs take into account both sources of uncertainty[53,61].

Sensitivity analysis

For sensitivity analysis, modeling selections were tested by adjusting the lag days, the number of knots in the exposure–response function, the df for the seasonal and long-term time trends and the confounding effects of air pollutants. By varying the above parameters, we observed that the principal findings of this investigation remained robust, exhibiting negligible alterations (Supplementary Table 4). We also tested other WBGT indicators (daily maximum and minimum WBGT) in the model and found stable results consistent with the daily mean WBGT (Supplementary Table 5).

All the statistical analyses were performed in Python (v.3.9) and R software (v.4.2.1) with the dlnm and splines packages. A two-sided P value of <0.05 was considered statistically significant.

Reporting summary

Further information on research design is available in the Nature Portfolio Reporting Summary linked to this article.

Data availability

The climate data that support the findings of this study are openly available. The ERA5-Land reanalysis data are available at ECMWF website (https://cds.climate.copernicus.eu/). The CMIP6 climate projection data are available at the ESGF data portal (https://esgf-node.llnl.gov/search/cmip6/). The projected yearly city-level, provincial and national population by age and sex under 15 scenarios for China from 2010 to 2100 are all available at the Tsinghua Cloud (https://cloud.tsinghua.edu.cn/f/d593f46793fb4145b8b9/?dl=1). The dataset for the distribution of population density in Shanghai is available from the LandScan Program (LandScan Global 2023, Oak Ridge National Laboratory, https://doi.org/10.48690/1529167). We have published the dataset used to generate the conclusions of this study on Zenodo (https://zenodo.org/records/17016368)[76]. Data from the SHIB were collected under a data-sharing agreement and cannot be made publicly available. Access to the medical data may be granted for academic research purposes upon reasonable request to the corresponding author.

Code availability

Custom code that supports the findings of this study is available from the corresponding author upon request.

References

1. McMichael, A. J., Woodruff, R. E. & Hales, S. Climate change and human health: present and future risks. *Lancet* **367**, 859–869 (2006).
2. Watts, N. et al. Health and climate change: policy responses to protect public health. *Lancet* **386**, 1861–1914 (2015).
3. Berry, H. L., Bowen, K. & Kjellstrom, T. Climate change and mental health: a causal pathways framework. *Int. J. Public Health* **55**, 123–132 (2010).
4. Cianconi, P., Betrò, S. & Janiri, L. The impact of climate change on mental health: a systematic descriptive review. *Front. Psychiatry* **11**, 74 (2020).
5. Ouyang, H., Tang, X. & Zhang, R. Research themes, trends and future priorities in the field of climate change and health: a review. *Atmosphere* **13**, 2076 (2022).
6. Pörtner, H.-O. et al. (eds) in *Climate Change 2022: Impacts, Adaptation and Vulnerability* (eds H.-O. Pörtner et al.) 3–33 (IPCC, Cambridge Univ. Press, 2022).
7. Peng, Z., Wang, Q., Kan, H., Chen, R. & Wang, W. Effects of ambient temperature on daily hospital admissions for mental disorders in Shanghai, China: a time-series analysis. *Sci. Total Environ.* **590**, 281–286 (2017).
8. Almendra, R., Loureiro, A., Silva, G., Vasconcelos, J. & Santana, P. Short-term impacts of air temperature on hospitalizations for mental disorders in Lisbon. *Sci. Total Environ.* **647**, 127–133 (2019).
9. Wang, X., Lavigne, E., Ouellette-kuntz, H. & Chen, B. E. Acute impacts of extreme temperature exposure on emergency room admissions related to mental and behavior disorders in Toronto, Canada. *J. Affect. Disord.* **155**, 154–161 (2014).
10. Obradovich, N., Migliorini, R., Paulus, M. P. & Rahwan, I. Empirical evidence of mental health risks posed by climate change. *Proc. Natl Acad. Sci. USA* **115**, 10953–10958 (2018).
11. Burke, M. et al. Higher temperatures increase suicide rates in the United States and Mexico. *Nat. Clim. Change* **8**, 723–729 (2018).
12. Zhou, Y. et al. Assessing the burden of suicide death associated with nonoptimum temperature in a changing climate. *JAMA Psychiatry* **80**, 488–497 (2023).
13. Schmeltz, M. T. & Gamble, J. L. Risk characterization of hospitalizations for mental illness and/or behavioral disorders with concurrent heat-related illness. *PLoS ONE* **12**, e0186509 (2017).
14. World Health Organization *Mental Disorders* https://www.who.int/en/news-room/fact-sheets/detail/mental-disorders (2022).
15. Ebi, K. L. et al. Hot weather and heat extremes: health risks. *Lancet* **398**, 698–708 (2021).
16. Mora, C. et al. Global risk of deadly heat. *Nat. Clim. Change* **7**, 501–506 (2017).
17. Liang, C. et al. The influence of humid heat on morbidity of megacity Shanghai in China. *Environ. Int.* **183**, 108424 (2024).
18. Russo, S., Sillmann, J. & Sterl, A. Humid heat waves at different warming levels. *Sci. Rep.* **7**, 7477 (2017).
19. Vida, S., Durocher, M., Ouarda, T. B. & Gosselin, P. Relationship between ambient temperature and humidity and visits to mental health emergency departments in Québec. *Psychiatr. Serv.* **63**, 1150–1153 (2012).
20. Hwong, A. R. et al. Climate change and mental health research methods, gaps, and priorities: a scoping review. *Lancet Planet. Health* **6**, e281–e291 (2022).

21. Bouchama, A. et al. Prognostic factors in heat wave-related deaths. *Arch. Intern. Med.* **167**, 2170–2176 (2007).
22. Page, L. A. & Howard, L. M. The impact of climate change on mental health (but will mental health be discussed at Copenhagen?). *Psychol. Med.* **40**, 177–180 (2010).
23. GBD 2019 Mental Disorders Collaborators Global, regional, and national burden of 12 mental disorders in 204 countries and territories, 1990–2019: a systematic analysis for the Global Burden of Disease Study 2019. *Lancet Psychiatry* **9**, 137–150 (2022).
24. Basu, R., Gavin, L., Pearson, D., Ebisu, K. & Malig, B. Examining the association between apparent temperature and mental health-related emergency room visits in California. *Am. J. Epidemiol.* **187**, 726–735 (2018).
25. Niu, Y. et al. Short-term effect of apparent temperature on daily emergency visits for mental and behavioral disorders in Beijing, China: a time-series study. *Sci. Total Environ.* **733**, 139040 (2020).
26. Min, M. et al. Effect of apparent temperature on daily emergency admissions for mental and behavioral disorders in Yancheng, China: a time-series study. *Environ. Health* **18**, 98 (2019).
27. Aguglia, A., Serafini, G., Escelsior, A., Amore, M. & Maina, G. What is the role of meteorological variables on involuntary admission in psychiatric ward? An Italian cross-sectional study. *Environ. Res.* **180**, 108800 (2020).
28. Zhao, L. et al. Interactions between urban heat islands and heat waves. *Environ. Res. Lett.* **13**, 034003 (2018).
29. Zhang, K. et al. Increased heat risk in wet climate induced by urban humid heat. *Nature* **617**, 738–742 (2023).
30. Epstein, Y. & Moran, D. S. Thermal comfort and the heat stress indices. *Ind. Health.* **44**, 388–398 (2006).
31. Li, D., Yuan, J. & Kopp, R. E. Escalating global exposure to compound heat–humidity extremes with warming. *Environ. Res. Lett.* **15**, 064003 (2020).
32. Knutson, T. R. & Ploshay, J. J. Detection of anthropogenic influence on a summertime heat stress index. *Clim. Change* **138**, 25–39 (2016).
33. Zhang, S. et al. City-level population projection for China under different pathways from 2010 to 2100. *Sci. Data* **10**, 809 (2023).
34. Peng, X. China's demographic history and future challenges. *Science* **333**, 581–587 (2011).
35. Okamoto-Mizuno, K. & Mizuno, K. Effects of thermal environment on sleep and circadian rhythm. *J. Physiol. Anthropol.* **31**, 14 (2012).
36. Obradovich, N., Migliorini, R., Mednick, S. C. & Fowler, J. H. Nighttime temperature and human sleep loss in a changing climate. *Sci. Adv.* **3**, e1601555 (2017).
37. Nori-Sarma, A. et al. Association between ambient heat and risk of emergency department visits for mental health among US adults, 2010 to 2019. *JAMA Psychiatry.* **79**, 341–349 (2022).
38. Liu, J. et al. Is there an association between hot weather and poor mental health outcomes? A systematic review and meta-analysis. *Environ. Int.* **153**, 106533 (2021).
39. Pigeon, W. R., Pinquart, M. & Conner, K. Meta-analysis of sleep disturbance and suicidal thoughts and behaviors. *J. Clin. Psychiatry* **73**, e1160–e1167 (2012).
40. Hajdu, T. Temperature exposure and sleep duration: evidence from time use surveys. *Econ. Hum. Biol.* **54**, 101401 (2024).
41. Webb, W. L. Jr & Gehi, M. Electrolyte and fluid imbalance: neuropsychiatric manifestations. *Psychosomatics* **22**, 199–203 (1981).
42. Powle, H., et al. Identification of risk factors associated with hyponatremia in psychiatric patients: a case–control study. *Med. Pharm. Rep.* **95**, 430–437 (2022).
43. Gędek, A. et al. Electrolyte disturbances related to sodium and potassium and electroconvulsive therapy: a systematic review. *J. Clin. Med.* **12**, 6677 (2023).
44. Weng, H. et al. Humid heat environment causes anxiety-like disorder via impairing gut microbiota and bile acid metabolism in mice. *Nat. Commun.* **15**, 5697 (2024).
45. Shiloh, R. et al. Abnormal thermoregulation in drug-free male schizophrenia patients. *Eur. Neuropsychopharmacol.* **11**, 285–288 (2001).
46. Schwaninger, M., Weisbrod, M., Schwab, S., Schroder, M. & Hacke, W. Hypothermia induced by atypical neuroleptics. *Clin. Neuropharmacol.* **21**, 344–346 (1998).
47. Yuan, J. et al. Relationship between temperature, dopaminergic neurotoxicity, and plasma drug concentrations in methamphetamine-treated squirrel monkeys. *J. Pharmacol. Exp. Ther.* **316**, 1210–1218 (2006).
48. Martin-Latry, K. et al. Psychotropic drugs use and risk of heat-related hospitalisation. *Eur. Psychiatry* **22**, 335–338 (2007).
49. Hansen, A. et al. The effect of heat waves on mental health in a temperate Australian city. *Environ. Health Perspect.* **116**, 1369–1375 (2008).
50. Bark, N. Deaths of psychiatric patients during heat waves. *Psychiatr. Serv.* **49**, 1088–1090 (1998).
51. Semenza, J. C., McCullough, J. E., Flanders, W. D., McGeehin, M. A. & Lumpkin, J. R. Excess hospital admissions during the July 1995 heat wave in Chicago. *Am. J. Prev. Med.* **16**, 269–277 (1999).
52. Goldberg, M. S., Gasparrini, A., Armstrong, B. & Valois, M. F. The short-term influence of temperature on daily mortality in the temperate climate of Montreal, Canada. *Environ. Res.* **111**, 853–860 (2011).
53. Gasparrini, A. et al. Projections of temperature-related excess mortality under climate change scenarios. *Lancet Planet. Health* **1**, e360–e367 (2017).
54. Martínez-Solanas, È et al. Projections of temperature-attributable mortality in Europe: a time series analysis of 147 contiguous regions in 16 countries. *Lancet Planet. Health* **5**, e446–e454 (2021).
55. *Shanghai Statistical Bulletin on National Economic and Social Development* https://tjj.sh.gov.cn/tjgb/20240321/f66c5b25ce604a1f9af755941d5f454a.html (Shanghai Municipal Statistics Bureau, 2023).
56. Cao, J. et al. Association of ambient air pollution with hospital outpatient and emergency room visits in Shanghai, China. *Sci. Total Environ.* **407**, 5531–5536 (2009).
57. Tebaldi, C. et al. Climate model projections from the Scenario Model Intercomparison Project (ScenarioMIP) of CMIP6. *Earth Syst. Dynam.* **12**, 253–293 (2021).
58. O'Neill, B. C. et al. The Scenario Model Intercomparison Project (ScenarioMIP) for CMIP6. *Geosci. Model Dev.* **9**, 3461–3482 (2016).
59. Riahi, K. et al. The Shared Socioeconomic Pathways and their energy, land use, and greenhouse gas emissions implications: an overview. *Glob. Environ. Change* **42**, 153–168 (2017).
60. Hempel, S., Frieler, K., Warszawski, L., Schewe, J. & Piontek, F. A trend-preserving bias correction—the ISI-MIP approach. *Earth Syst. Dyn.* **4**, 219–236 (2013).
61. Vicedo-Cabrera, A. M., Sera, F. & Gasparrini, A. Hands-on tutorial on a modeling framework for projections of climate change impacts on health. *Epidemiology* **30**, 321–329 (2019).
62. Parsons, L. A., Shindell, D., Tigchelaar, M., Zhang, Y. & Spector, J. T. Increased labor losses and decreased adaptation potential in a warmer world. *Nat. Commun.* **12**, 7286 (2021).
63. Liljegren, J. C., Carhart, R. A., Lawday, P., Tschopp, S. & Sharp, R. Modeling the wet bulb globe temperature using standard meteorological measurements. *J. Occup. Environ. Hyg.* **5**, 645–655 (2008).

64. *Shanghai Population Census Yearbook* https://tjj.sh.gov.cn/tjnj_rkpc/20220829/734169a3ce96405e88917bebd78376bf.html (Leading Group office of Shanghai for the Seventh National Population Census and Shanghai Municipal Bureau of Statistics, 2020).
65. Iribarne, J. V. & Godson, W. L. *Atmospheric Thermodynamics* Vol. 6 (Springer, 2012).
66. Davies-Jones, R. An efficient and accurate method for computing the wet-bulb temperature along pseudoadiabats. *Mon. Weather Rev.* **136**, 2764–2785 (2008).
67. Lee, S., Lee, H., Myung, W., Kim, E. J. & Kim, H. Mental disease-related emergency admissions attributable to hot temperatures. *Sci. Total Environ.* **616**, 688–694 (2018).
68. Gasparrini, A. & Armstrong, B. Time series analysis on the health effects of temperature: advancements and limitations. *Environ. Res.* **110**, 633–638 (2010).
69. Gasparrini, A. Modeling exposure–lag–response associations with distributed lag non-linear models. *Stat. Med.* **33**, 881–899 (2014).
70. Kim, Y., Kim, H. & Kim, D. S. Association between daily environmental temperature and suicide mortality in Korea (2001–2005). *Psychiatry Res.* **186**, 390–396 (2011).
71. Liu, X., Liu, H., Fan, H., Liu, Y. & Ding, G. Influence of heat waves on daily hospital visits for mental illness in Jinan, China—a case-crossover study. *Int. J. Environ. Res. Public Health* **16**, 87 (2019).
72. Gasparrini, A. & Armstrong, B. The impact of heat waves on mortality. *Epidemiology* **22**, 68–73 (2011).
73. Gasparrini, A. Distributed lag linear and non-linear models in R: the package dlnm. *J. Stat. Softw.* **43**, 1–20 (2011).
74. McGregor, G. R. & Vanos, J. K. Heat: a primer for public health researchers. *Public Health* **161**, 138–146 (2017).
75. Zhao, Q. et al. Global, regional, and national burden of mortality associated with non-optimal ambient temperatures from 2000 to 2019: a three-stage modelling study. *Lancet Planet. Health* **5**, e415–e425 (2021).
76. Liang, C. Replication data for 'Projecting the morbidity burden of mental and behavioral disorders associated with increasing humid heat in Shanghai'. *Zenodo* https://zenodo.org/records/17016368 (2025).

Acknowledgements

This research was supported by the National Natural Science Foundation of China (grants 42288101 and 42175066) and Shanghai International Science and Technology Partnership Project (grant 21230780200). G.S. is supported by the China Brain Project (grant 2025ZD0215100), the National Natural Science Foundation of China (grant 82150710554), the Chinese National Key Project (grant 2023YFE0199700), the National Natural Science Foundation of China (grant W2541022) and the EC Horizon Europe: environMENTAL project.

Author contributions

J.Y. designed and supervised the research. C.L. developed the modeling framework and conducted the analyses. C.L. and J.Y. wrote the original draft. G.S., R.Z. and X.T. provided constructive comments to improve the manuscript. All authors edited and finally approved the manuscript.

Competing interests

The authors declare no competing interests.

Additional information

Extended data is available for this paper at https://doi.org/10.1038/s44220-025-00519-y.

Supplementary information The online version contains supplementary material available at https://doi.org/10.1038/s44220-025-00519-y.

Correspondence and requests for materials should be addressed to Jiacan Yuan.

Peer review information *Nature Mental Health* thanks Aleš Urban and the other, anonymous, reviewer(s) for their contribution to the peer review of this work.

the environMENTAL Consortium

Esther Hitchen[7,10], Elli Polemiti[7,10], Emin Serin[10], Hedi Kebir[7,10], Tristram A. Lett[7,10], Nilakshi Vaidya[7,10], Jean-Charles Roy[7,10], Henrik Walter[10,11], Andreas Heinz[10,11], Markus Ralser[12,13,14], Sven Twardziok[15], Roland Eils[15], Marcel Jentsch[15], Ulrike-Helene Taron[15], Tatjana Schütz[15], Kerstin Schepanski[16], Tobias Banaschewski[17,18], Maja Neidhart[10,17], Andreas Meyer-Lindenberg[18,19], Heike Tost[18,19], Nathalie Holz[17,18], Emanuel Schwarz[18,19,20], Argyris Stringaris[17], Nina Christmann[17], Karina Janson[17,21], Frauke Nees[21], Maja Neidhart[21], Beke Seefried[21], Rieke Aden[21], Ole A. Andreassen[22], Lars T. Westlye[22,23], Dennis van der Meer[22], Sara Fernández-Cabello[22,23], Rikka Kjelkenes[22,23], Helga Ask[23,24], Michael Rapp[25], Mira Tschorn[25], Sarah Jane Böttger[25], Andre Marquand[26], Antoine Bernas[26], Gaia Novarino[27], Mel Slater[28], Jaime Gallego[28], Álvaro Pastor[28], Guillem Feixas[28], Francisco José Eiroa-Orosa[28], Markus M. Nöthen[29], Andreas J. Forstner[29], Isabelle Claus[29], Carina Mathey[29], Stefanie Heilmann-Heimbach[29,30], Per Hoffmann[29,30], Abigail Miller[29,30], Peter Sommer[31], Karen Schmitt[31], Johannes Wilbertz[31], Myrto Patraskaki[31], Viktor Jirsa[32], Spase Petkoski[32], Anastasios-Polykarpos Athanasiadis[32], Bernhard Spanlang[33], Charlie Pearmund[33], Sören Hese[34], Paul Renner[16,34], Tianye Jia[35], Xiao Chang[35], Yuxiang Dai[36], Yunman Xia[36], Yuzhu Li[36], Yanqing Zhang[36], Vince Calhoun[37], Paul Thompson[38], Nicholas Clinton[39], Sylvane Desrivières[40], Kofoworola Agunbiade[40], Xinyang Yu[40], Zuo Zhang[40,41], Di Chen[40], Allan H. Young[42], Ameli Schwalber[43], Vanessa Köhler[43], Bernd Stahl[44], George Ogoh[44], Tamara Schikowski[45] & Ragnhild Brandlistuen[46]

[10]Department of Psychiatry and Psychotherapy, Charite-Universitaetsmedizin Berlin, Berlin, Germany. [11]German Center for Mental Health (DZPG), University Berlin-Potsdam, Berlin, Germany. [12]Department of Biochemistry, Charite-Universitaetsmedizin Berlin, Berlin, Germany. [13]Nuffield Department of Medicine, University of Oxford, Oxford, UK. [14]Max Planck Institute for Molecular Genetics, Berlin, Germany. [15]Berlin Institute of Health, Charité-Universitätsmedizin Berlin, Berlin, Germany. [16]Institute of Meteorology, Freie Universität Berlin, Berlin, Germany. [17]Department of Child and Adolescent Psychiatry and Psychotherapy, Central Institute of Mental Health, Medical Faculty Mannheim, Heidelberg University, Mannheim, Germany. [18]German Center for Mental Health (DZPG), Mannheim, Germany. [19]Department of Psychiatry and Psychotherapy, Central Institute of Mental Health, Medical Faculty Mannheim, Heidelberg University, Mannheim, Germany. [20]Hector Institute for Artificial Intelligence in Psychiatry, Central Institute of Mental Health, Medical Faculty Mannheim, Heidelberg University, Mannheim, Germany. [21]Institute of Medical Psychology and Medical Sociology, University Medical Center Schleswig-Holstein, Kiel University, Kiel, Germany. [22]Centre for Precision Psychiatry, Division of Mental Health and Addiction, Oslo University Hospital & Institute of Clinical Medicine, University of Oslo, Oslo, Norway. [23]Department of Psychology, University of Oslo, Oslo, Norway. [24]PsychGen Centre for Genetic Epidemiology and Mental Health, Norwegian Institute of Public Health, Oslo, Norway. [25]Social and Preventive Medicine, University of Potsdam, Potsdam, Germany. [26]Cognitive Neuroscience, Radboud University Medical Centre, Nijmegen, The Netherlands. [27]Institute of Science and Technology Austria, Vienna, Austria. [28]Department of Clinical Psychology and Psychobiology, Event Lab, Institute of Neurosciences, University of Barcelona, Barcelona, Spain. [29]Institute of Human Genetics, School of Medicine and University Hospital Bonn, University of Bonn, Bonn, Germany. [30]Life and Brain GmbH, Bonn, Germany. [31]Ksilink, Strasbourg, France. [32]Institut de Neurosciences des Systèmes (INS) UMR1106, Aix Marseille Université, Institut National de la Santé et de la Recherche Médicale (Inserm), Marseille, France. [33]Virtual Bodyworks, Barcelona, Spain. [34]Department of Earth Observation, Friedrich Schiller University Jena, Jena, Germany. [35]Institute of Science and Technology for Brain-Inspired Intelligence, Fudan University, Shanghai, China. [36]Fudan University, Shanghai, China. [37]Tri-institutional Center for Translational Research in Neuroimaging and Data Science (TReNDS), Georgia State University, Georgia Institute of Technology and Emory University, Atlanta, GA, USA. [38]Stevens Neuroimaging & Informatics Institute, Keck School of Medicine, University of Southern California, Los Angeles, CA, USA. [39]Google, Inc., Mountain View, CA, USA. [40]Social, Genetic and Developmental Psychiatry Centre, Institute of Psychiatry, Psychology & Neuroscience, King's College London, London, UK. [41]Institute for Mental Health, School of Psychology, University of Birmingham, Birmingham, UK. [42]Psychological Medicine, King's College London, South London & Maudsley NHS Foundation Trust, London, UK. [43]concentris research management gmbh, Fürstenfeldbruck, Germany. [44]School of Computer Science, University of Nottingham, Nottingham, UK. [45]IUF Leibniz Research Institute for Environmental Medicine, Düsseldorf, Germany. [46]The Norwegian Mother, Father and Child Cohort Study, Norwegian Institute of Public Health, Oslo, Norway.

https://doi.org/10.1038/s44220-025-00519-y

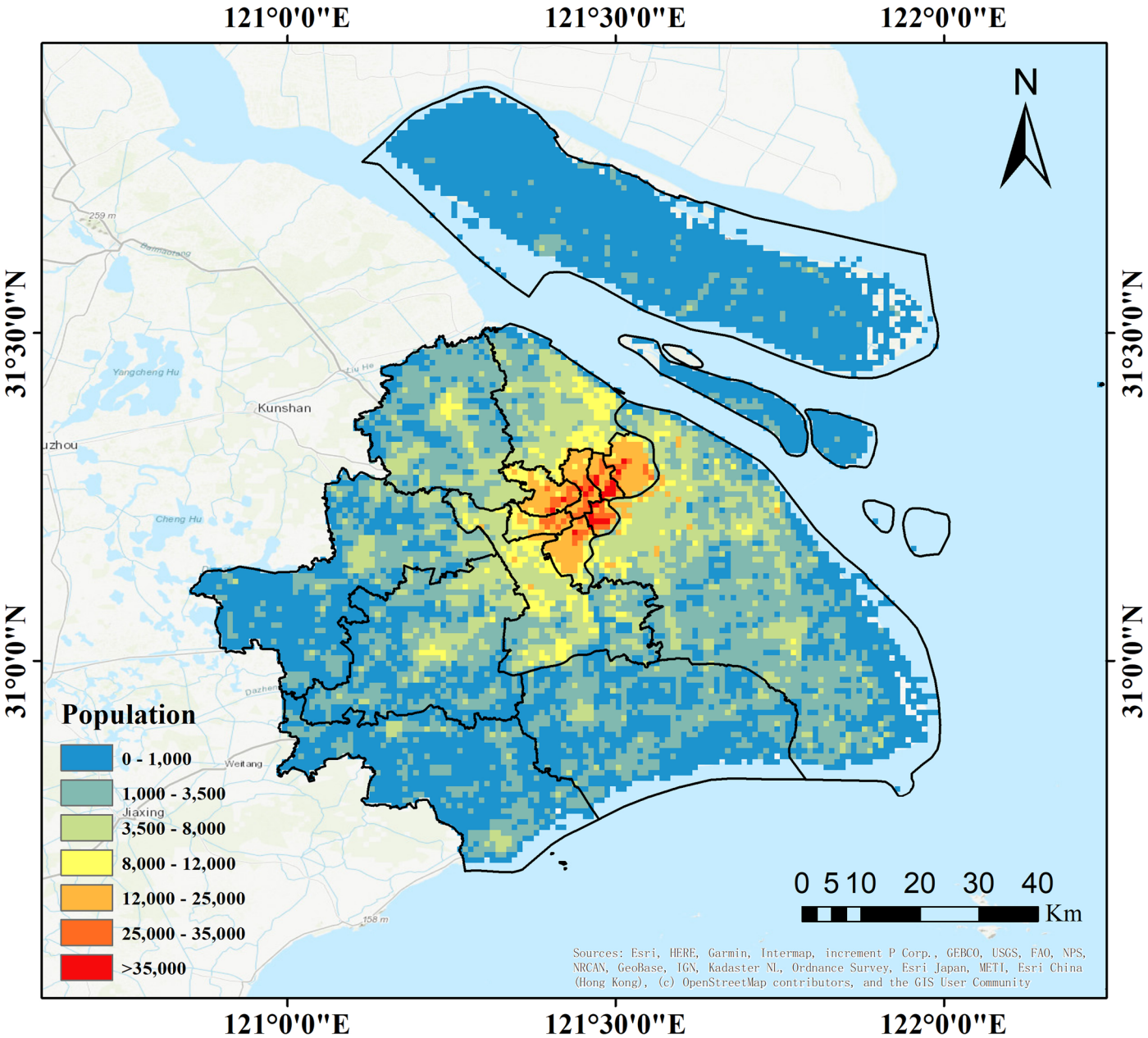

Extended Data Fig. 1 | Location of the study area: the city of Shanghai. The population density is shown in the shaded area. (Data Source: https://landscan.ornl.gov/).

https://doi.org/10.1038/s44220-025-00519-y

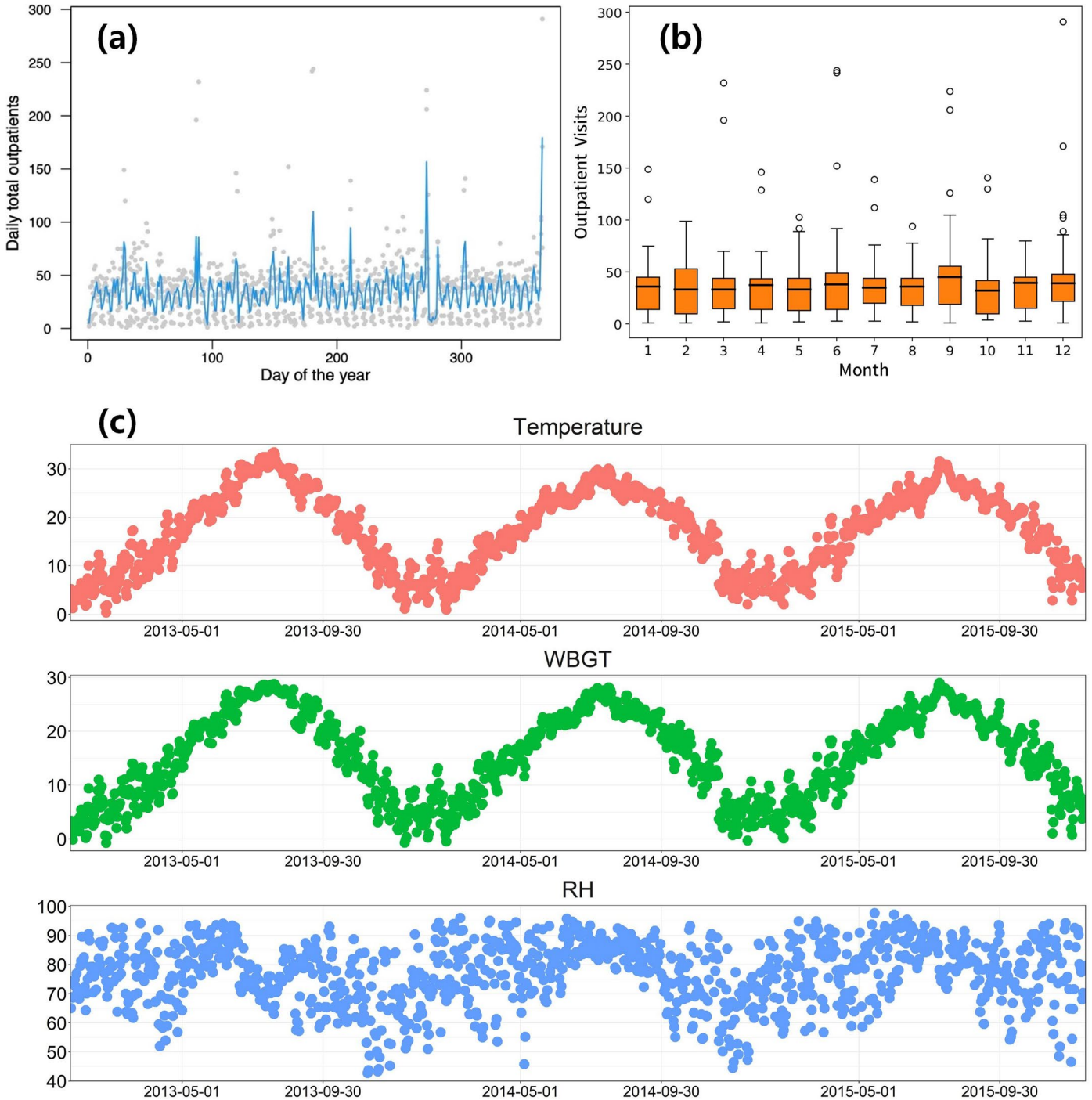

Extended Data Fig. 2 | Seasonal trends of the observed daily hospital admissions and meteorological variables in Shanghai between 2013 and 2015. (**a**) Gray dots correspond to the daily hospital admissions for MBDs registered in each day of the year. The blue line depicts the mean number of cases per day of the year. (**b**) Monthly distribution characteristics of daily hospital admissions in Shanghai. The box plots show the median (line), 25%-75% range (box), 5-95% range (whiskers), and the outliers (circles). (**c**) The time series of daily mean temperature, WBGT and relative humidity (RH) in the warm season of Shanghai.

https://doi.org/10.1038/s44220-025-00519-y

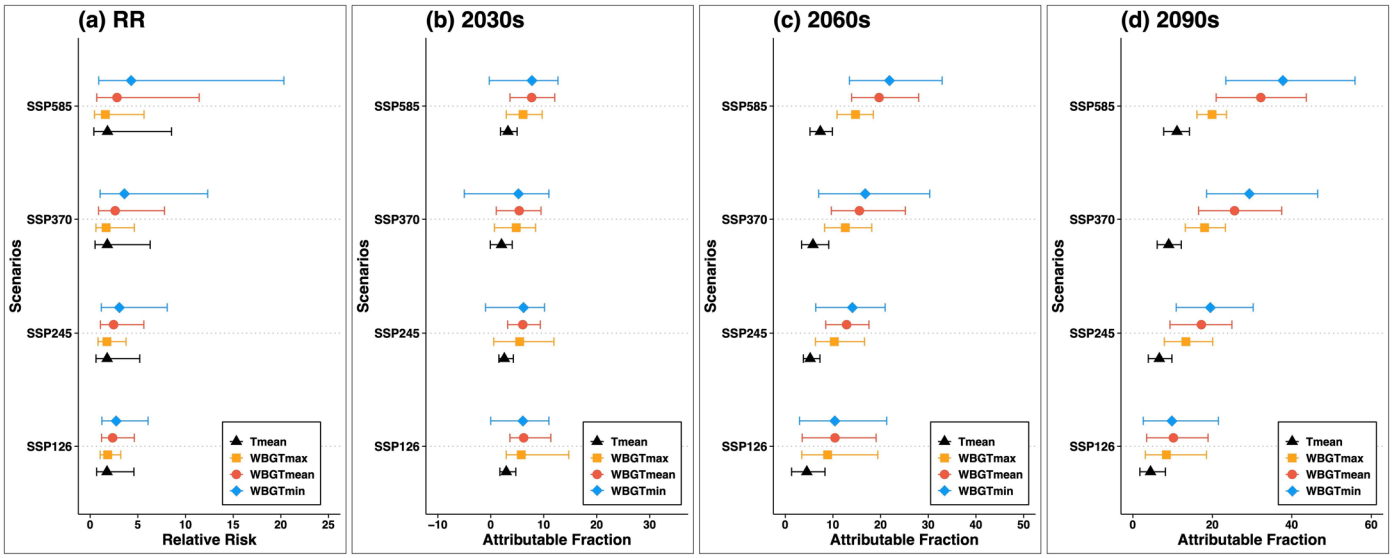

Extended Data Fig. 3 | Projected relative risk and morbidity burden exclusively driven by climate warming. (**a**) The projected relative risk (RR) at extreme heat (99th ambient temperature/ WBGT percentile) in the 2090s, and the attributable fraction of MBDs hospital admissions due to T_{mean} (black), $WBGT_{mean}$ (orange), $WBGT_{max}$ (red) and $WBGT_{min}$ (blue) in (**b**) the 2030s, (**c**) the 2060s and (**d**) the 2090s compared to the reference period (2010–19) in Shanghai by different SSPs.

https://doi.org/10.1038/s44220-025-00519-y

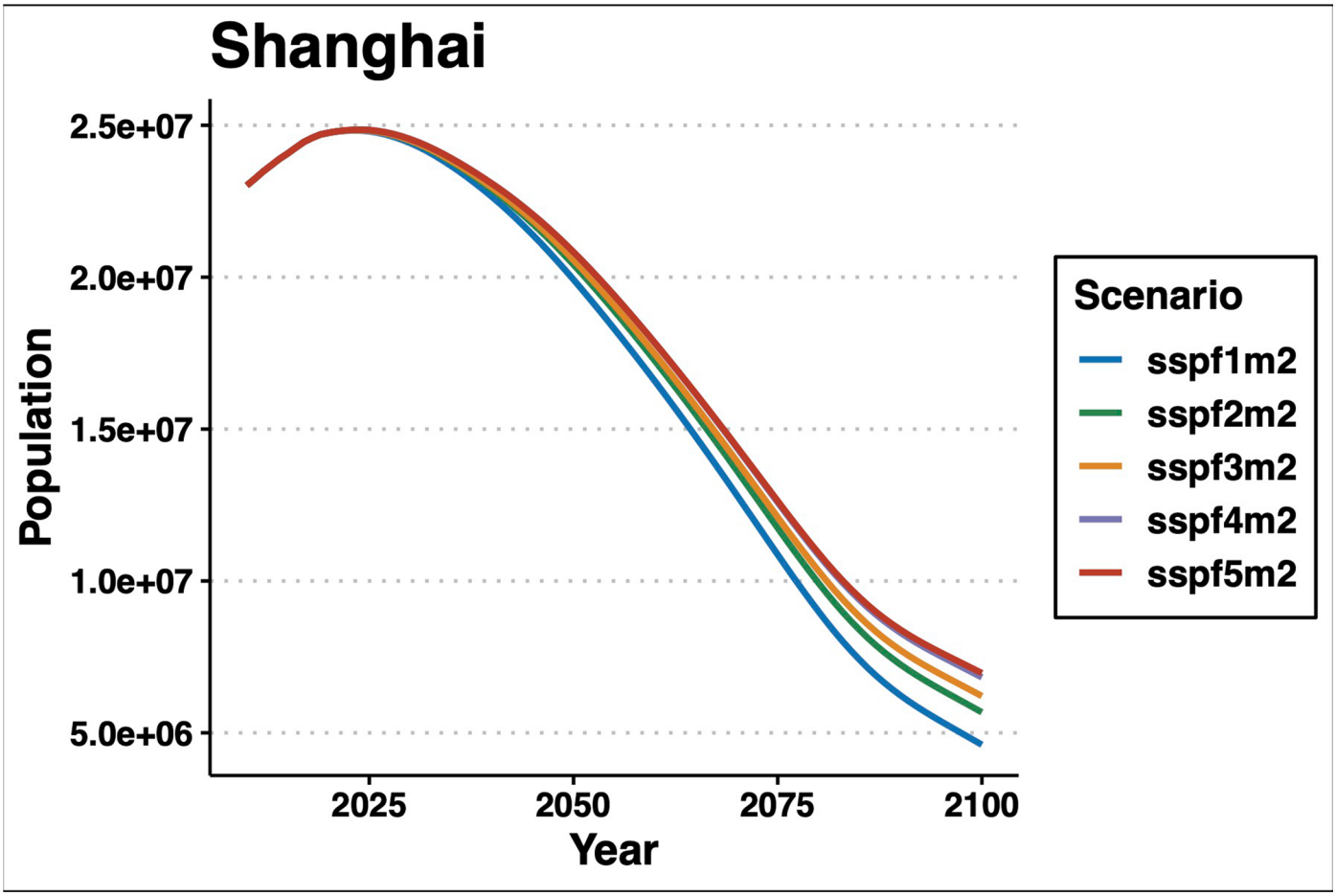

Extended Data Fig. 4 | Future population changes at the city level from 2010 to 2100 under five fertility scenarios in Shanghai. The blue, green, orange, purple and red lines respectively represent the five selected fertility scenarios (Fer1 to Fer5) and the moderate migration scenario (Migr2) for Shanghai.

https://doi.org/10.1038/s44220-025-00519-y

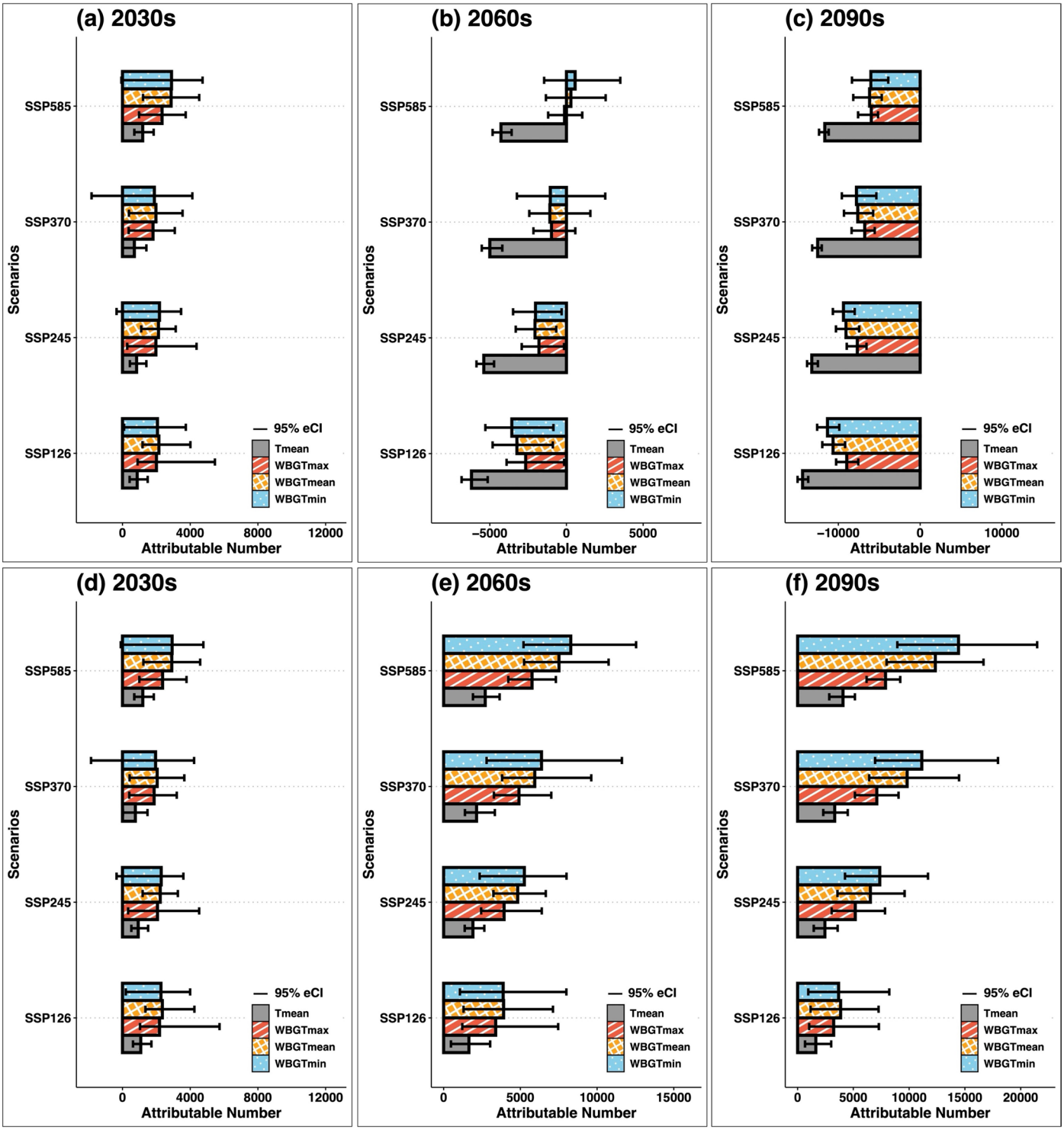

Extended Data Fig. 5 | Heat-attributable MBDs hospital admissions under four GHG-emission scenarios relative to the reference period (2010-19), considering population change effects or not. The projected number of heat-attributable MBDs hospital admissions due to T_{mean}, $WBGT_{mean}$, $WBGT_{max}$ and $WBGT_{min}$ in 2030s, 2060s and 2090s compared to the reference period (2010-19) in Shanghai by different SSPs with (**a**–**c**) and without (**d**–**f**) population change.

https://doi.org/10.1038/s44220-025-00519-y

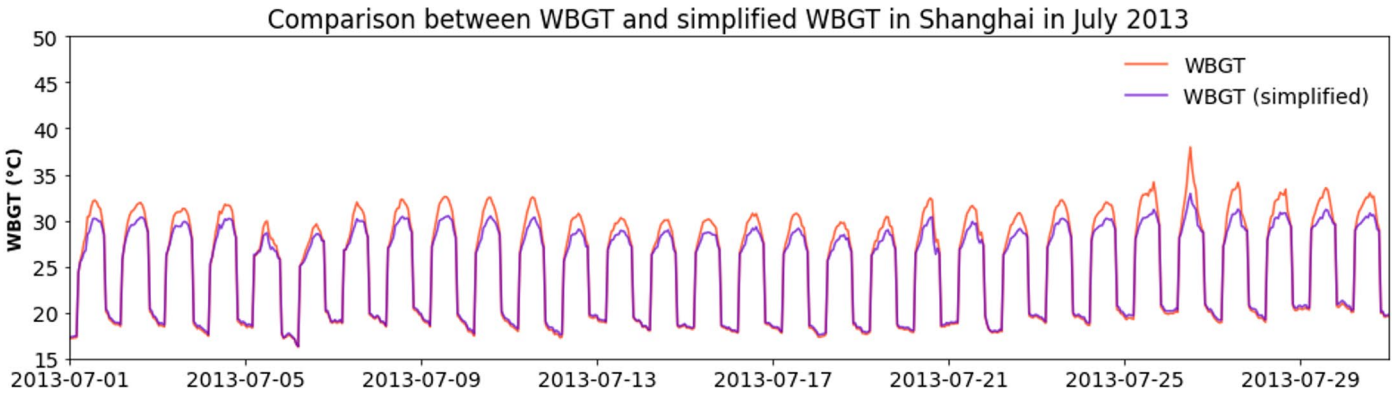

Extended Data Fig. 6 | Comparison between WBGT and simplified WBGT in Shanghai during July 2013 based on ERA5 re-analysis data. The orange and purple lines represent the original WBGT and the simplified version of WBGT, respectively.

https://doi.org/10.1038/s44220-025-00519-y

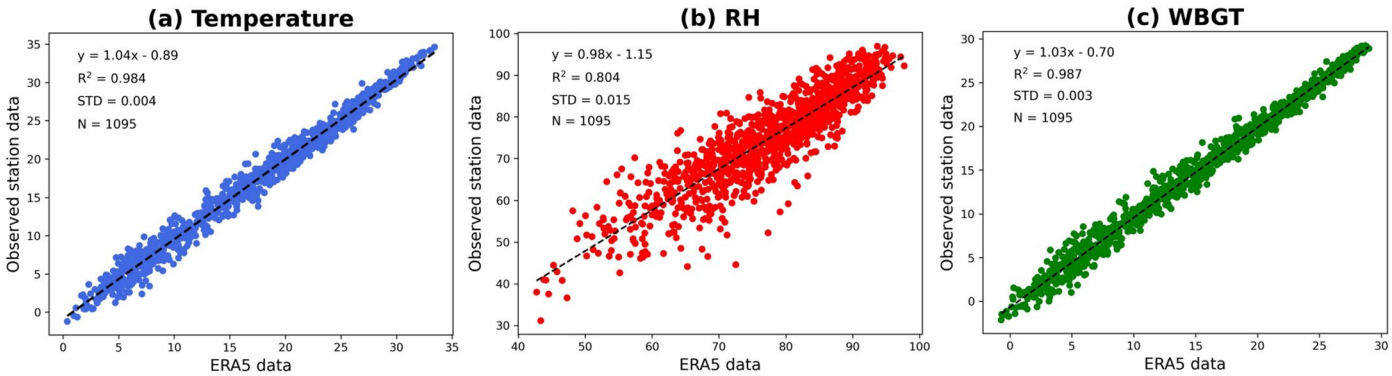

Extended Data Fig. 7 | ERA5 re-analysis data showed good correlation with site observation data. The scatterplot for (**a**) temperature, (**b**) relative humidity and (**c**) WBGT between the site observations and ERA5-derived data (significant test P = 0.01). The black dashed line is the fitted line from linear regression. The regression equations and coefficients of determination (R^2) are given, as well as the standard errors (STD).

https://doi.org/10.1038/s44220-025-00519-y

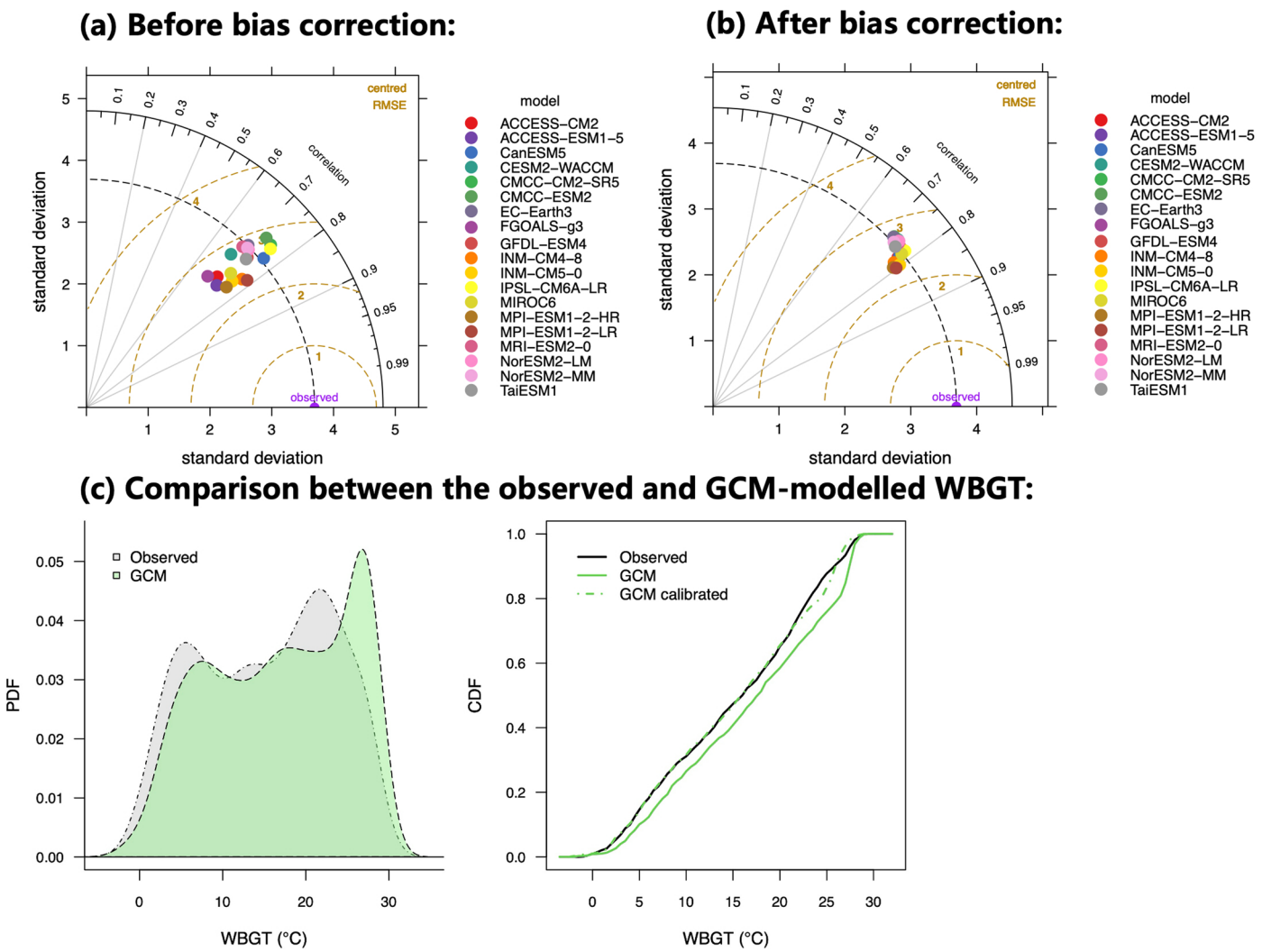

Extended Data Fig. 8 | Comparison between observed WBGT and GCM-modelled WBGT, before and after bias correction. The Taylor Diagrams present comparisons of the observed WBGT series with 19 GCM-modelled WBGT series before (**a**) and after (**b**) bias correction. (**c**) Comparison of the distribution of probabilistic density (PDF, left panel) and distribution of cumulative density function (CDF, right panel) between the raw and the bias-corrected modelled WBGT. The CDF of observed WBGT is shown as black line in the right panel.

https://doi.org/10.1038/s44220-025-00519-y

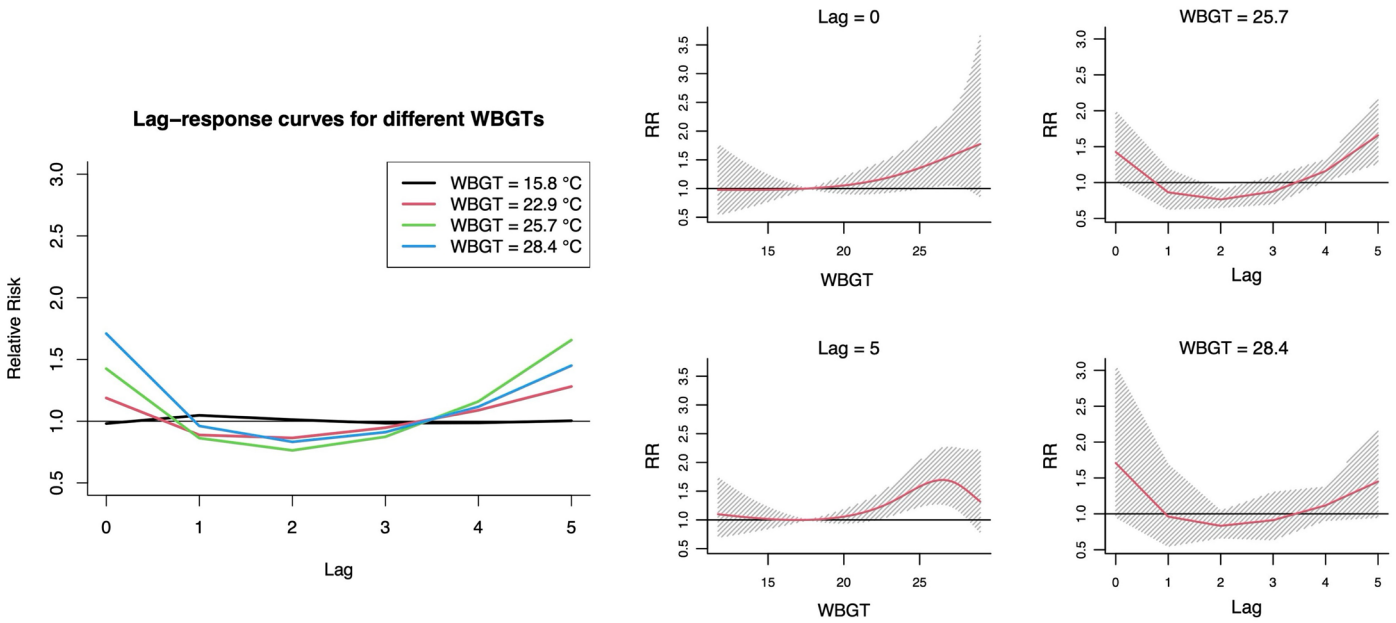

Extended Data Fig. 9 | The lag structure for the relative risks (RRs) of MBDs hospital admissions associated with $WBGT_{mean}$ in Shanghai. Left panel: Lag-response curves for WBGTs at different cut-off points specific to mild and extreme humid hot circumstance. The black, red, green and blue lines represent the 1st, 50th, 75th and 99th percentiles of WBGT in the warm season of Shanghai. Right panel: Depicts both exposure–response relationships specific to lag 0 and 5 (left column), and lag–response relationships specific to WBGTs 25.7°C and 28.4°C (right column).

https://doi.org/10.1038/s44220-025-00519-y

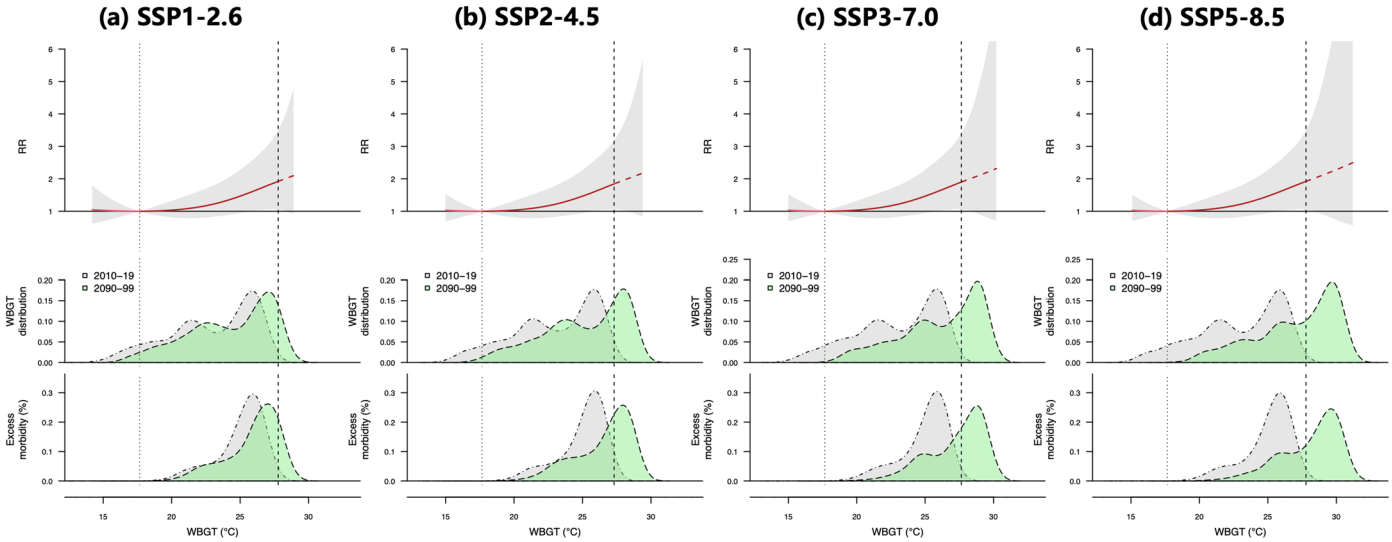

Extended Data Fig. 10 | Daily mean WBGT and excess morbidity for MBDs hospital admissions in Shanghai for present and future periods. Comparison of projected RRs, modeled WBGTs and related excess morbidity for present (2010-19) and future (2090-99) periods under (a) SSP1-2.6, (b) SSP2-4.5, (c) SSP3-7.0 and (d) SSP5-8.5 scenario, respectively. Top panel: exposure–response curve represented as morbidity RR across the WBGT (°C) range, with 95% empirical confidence intervals (gray area). The doted vertical line corresponds to the minimum morbidity WBGT (MMT). The dashed part of the curve represents the extrapolation beyond the maximum WBGT observed in 2010-19 (dashed vertical line). Mid panel: distribution of the CMIP6-modeled WBGT for the current (2010-19, gray area) and at the end of the century (2090-99, green area), projected using 19 CMIP6 GCMs and four scenarios (SSP1-2.6, SSP2-4.5, SSP3-7.0, SSP5-8.5). Bottom panel: the related distribution of excess morbidity, expressed as the fraction of additional hospitalizations (%) attributed to high WBGTs compared with MMT.

nature portfolio

Corresponding author(s): Jiacan Yuan

Last updated by author(s): Sep 1, 2025

Reporting Summary

Nature Portfolio wishes to improve the reproducibility of the work that we publish. This form provides structure for consistency and transparency in reporting. For further information on Nature Portfolio policies, see our Editorial Policies and the Editorial Policy Checklist.

Statistics

For all statistical analyses, confirm that the following items are present in the figure legend, table legend, main text, or Methods section.

n/a	Confirmed
☐	☒ The exact sample size (*n*) for each experimental group/condition, given as a discrete number and unit of measurement
☐	☒ A statement on whether measurements were taken from distinct samples or whether the same sample was measured repeatedly
☐	☒ The statistical test(s) used AND whether they are one- or two-sided *Only common tests should be described solely by name; describe more complex techniques in the Methods section.*
☐	☒ A description of all covariates tested
☐	☒ A description of any assumptions or corrections, such as tests of normality and adjustment for multiple comparisons
☐	☒ A full description of the statistical parameters including central tendency (e.g. means) or other basic estimates (e.g. regression coefficient) AND variation (e.g. standard deviation) or associated estimates of uncertainty (e.g. confidence intervals)
☐	☒ For null hypothesis testing, the test statistic (e.g. *F*, *t*, *r*) with confidence intervals, effect sizes, degrees of freedom and *P* value noted *Give P values as exact values whenever suitable.*
☐	☒ For Bayesian analysis, information on the choice of priors and Markov chain Monte Carlo settings
☐	☒ For hierarchical and complex designs, identification of the appropriate level for tests and full reporting of outcomes
☐	☒ Estimates of effect sizes (e.g. Cohen's *d*, Pearson's *r*), indicating how they were calculated

Our web collection on statistics for biologists contains articles on many of the points above.

Software and code

Policy information about availability of computer code

Data collection	The climate data that support the findings of this study are openly available. ERA-5 reanalysis data is available at ECMWF website (https://cds.climate.copernicus.eu/). The data of CMIP6 climate projections is available at ESGF data portal (https://esgf-node.llnl.gov/search/cmip6/). The projected yearly city-level, provincial and national population by age, sex, under 15 scenarios for China from 2010 to 2100 are all available at the Tsinghua Cloud (https://cloud.tsinghua.edu.cn/f/d593f46793fb4145b8b9/?dl=1). The dataset for the distribution of population density in Shanghai is available from LandScan Program (LandScan Global 2023, Oak Ridge National Laboratory, https://doi.org/10.48690/1529167). The datasets generated or analyzed during the current study for Main Figures and Extended Data Figures have been published on Zenodo (https://zenodo.org/records/17016368). The morbidity data from Shanghai Health Insurance Bureau is subject to institutional data use agreements and confidentiality protocols that restrict public sharing. As such, the data cannot be deposited in a public repository. Access to the medical data may be granted for academic research purposes upon reasonable request from the corresponding author.
Data analysis	Statistical analyses were performed using Python (v3.9) and R software (v4.2.1) with 'dlnm' and 'splines' packages. Custom code that supports the findings of this study is available from the corresponding author upon request.

For manuscripts utilizing custom algorithms or software that are central to the research but not yet described in published literature, software must be made available to editors and reviewers. We strongly encourage code deposition in a community repository (e.g. GitHub). See the Nature Portfolio guidelines for submitting code & software for further information.

Data

Policy information about availability of data

All manuscripts must include a data availability statement. This statement should provide the following information, where applicable:

- Accession codes, unique identifiers, or web links for publicly available datasets
- A description of any restrictions on data availability
- For clinical datasets or third party data, please ensure that the statement adheres to our policy

The climate data that support the findings of this study are openly available. ERA-5 reanalysis data is available at ECMWF website (https://cds.climate.copernicus.eu/). The data of CMIP6 climate projections is available at ESGF data portal (https://esgf-node.llnl.gov/search/cmip6/). The projected yearly city-level, provincial and national population by age, sex, under 15 scenarios for China from 2010 to 2100 are all available at the Tsinghua Cloud (https://cloud.tsinghua.edu.cn/f/d593f46793fb4145b8b9/?dl=1). The dataset for the distribution of population density in Shanghai is available from LandScan Program (LandScan Global 2023, Oak Ridge National Laboratory, https://doi.org/10.48690/1529167). The datasets generated or analyzed during the current study for Main Figures and Extended Data Figures have been published on Zenodo (https://zenodo.org/records/17016368). Medical Data from Shanghai Health Insurance Bureau were collected under a data sharing agreement and cannot be made publicly available. Access to the data may be granted for academic purposes upon reasonable request from the corresponding author, in accordance with the terms of the original agreement.

Research involving human participants, their data, or biological material

Policy information about studies with human participants or human data. See also policy information about sex, gender (identity/presentation), and sexual orientation and race, ethnicity and racism.

Reporting on sex and gender	The information of sex and gender has not been collected in this study and were not considered in study design as well.
Reporting on race, ethnicity, or other socially relevant groupings	Information on race or ethnicity was not available in the dataset, as this information is not routinely collected in the Shanghai Health Insurance Bureau system. Data were analyzed at aggregate level and no participants were contacted.
Population characteristics	The study population consisted of hospitalized patients diagnosed with mental and behavioral disorders (F00–F99), as recorded in the Shanghai Health Insurance Bureau database between 2013 and 2015.
Recruitment	This was a retrospective study based on administrative health records. No participants were recruited prospectively. All data were anonymized prior to analysis. Consequently, questions regarding participant sex, age, informed consent, or compensation do not apply.
Ethics oversight	The study protocol was approved by the Institutional Review Board at the School of Public Health, Fudan University (No. 2021-04-0889). All analyses were conducted at the aggregate level and no participants were contacted.

Note that full information on the approval of the study protocol must also be provided in the manuscript.

Field-specific reporting

Please select the one below that is the best fit for your research. If you are not sure, read the appropriate sections before making your selection.

☐ Life sciences ☐ Behavioural & social sciences ☒ Ecological, evolutionary & environmental sciences

For a reference copy of the document with all sections, see nature.com/documents/nr-reporting-summary-flat.pdf

Ecological, evolutionary & environmental sciences study design

All studies must disclose on these points even when the disclosure is negative.

Study description	We utilized the Wet-Bulb Globe Temperature (WBGT) index as the metric to characterize the humid-heat exposure. The historical associations between daily mental and behavioral disorders hospitalizations and WBGT metrics were established using a Distributed Lag Non-linear Model (DLNM) during the warm season (May to September) from 2013 to 2015 in Shanghai, China. Future morbidity burden related to the combined effect of high temperature and humidity were projected under four greenhouse gas (GHG) emission scenarios (SSP1-2.6, SSP2-4.5, SSP3-7.0 and SSP5-8.5).
Research sample	The research sample consisted of anonymized inpatient records of individuals diagnosed with mental and behavioral disorders (ICD-10 codes F00–F99), obtained from the Shanghai Health Insurance database. The dataset includes information on hospital admission, and primary diagnosis. The study population covers a large, diverse urban population in Shanghai, China, and is representative of individuals receiving inpatient psychiatric care under the municipal health insurance system. The use of this dataset allows for large-scale, population-based analysis of hospital admissions related to mental health, particularly in response to environmental exposures. No direct manipulation or intervention was performed, as this was a retrospective observational study based on existing administrative data.
Sampling strategy	This study employed a retrospective, population-based sampling strategy. All inpatient records of individuals diagnosed with mental

Sampling strategy	and behavioral disorders (ICD-10 codes F00–F99) from the Shanghai Health Insurance database during the study period [2013–2015] were included. No sampling or exclusion criteria were applied apart from the diagnostic codes and data completeness. As the dataset covers a comprehensive population enrolled in the municipal insurance system, it provides a representative sample of psychiatric inpatients in Shanghai. The use of administrative data ensures large sample size and minimizes selection bias; however, information is limited to insured individuals and may not capture cases without insurance coverage.
Data collection	The data used in this study were obtained from the Shanghai Health Insurance database, an administrative claims database that routinely collects inpatient medical records for all insured individuals in Shanghai. Clinical and demographic information, including diagnoses (coded according to ICD-10), and admission dates, were recorded electronically by certified healthcare professionals at designated hospitals and submitted to the municipal health insurance system. No direct data collection was conducted by the study investigators.
Timing and spatial scale	The medical data span from January 2013 to December 2015 with daily interval, covering both hot and non-hot seasons. Heat exposure was assigned based on date of admissions. This work included all registered residents who participated in Shanghai Health Insurance System. The climate data covers historical period 2013-2015 from the observations, and future period 2015-2100 from CMIP6 archive.
Data exclusions	No data were excluded from the analyses. All available records meeting the inclusion criteria (i.e., diagnosis codes F00–F99) were retained and analyzed.
Reproducibility	All key methods, statistical models, and variable definitions are described in detail in the Methods section of the manuscript. The raw data of administrative health records from the Shanghai Health Insurance System database cannot be publicly shared due to privacy and regulatory restrictions. However, the analysis code and aggregated results are available from the corresponding author upon reasonable request. The procedures used for data cleaning, variable construction, and statistical modeling have been fully documented to ensure reproducibility of the findings.
Randomization	Randomization was not applicable in this study, as it was a retrospective observational analysis based on administrative health records. No experimental intervention or group assignment was performed. All analyses were conducted on naturally occurring, real-world inpatient data.
Blinding	Blinding was not applicable to this study. The analysis was based on de-identified administrative health records, with no intervention, treatment assignment, or direct interaction with participants. All data were anonymized prior to access, and outcome classification was determined using standard ICD-10 codes, reducing the potential for observer bias.

Did the study involve field work? ☐ Yes ☒ No

Reporting for specific materials, systems and methods

We require information from authors about some types of materials, experimental systems and methods used in many studies. Here, indicate whether each material, system or method listed is relevant to your study. If you are not sure if a list item applies to your research, read the appropriate section before selecting a response.

Materials & experimental systems

n/a	Involved in the study
☒	☐ Antibodies
☒	☐ Eukaryotic cell lines
☒	☐ Palaeontology and archaeology
☒	☐ Animals and other organisms
☒	☐ Clinical data
☒	☐ Dual use research of concern
☒	☐ Plants

Methods

n/a	Involved in the study
☒	☐ ChIP-seq
☒	☐ Flow cytometry
☒	☐ MRI-based neuroimaging

Plants

Seed stocks	*Report on the source of all seed stocks or other plant material used. If applicable, state the seed stock centre and catalogue number. If plant specimens were collected from the field, describe the collection location, date and sampling procedures.*
Novel plant genotypes	*Describe the methods by which all novel plant genotypes were produced. This includes those generated by transgenic approaches, gene editing, chemical/radiation-based mutagenesis and hybridization. For transgenic lines, describe the transformation method, the number of independent lines analyzed and the generation upon which experiments were performed. For gene-edited lines, describe the editor used, the endogenous sequence targeted for editing, the targeting guide RNA sequence (if applicable) and how the editor was applied.*
Authentication	*Describe any authentication procedures for each seed stock used or novel genotype generated. Describe any experiments used to assess the effect of a mutation and, where applicable, how potential secondary effects (e.g. second site T-DNA insertions, mosiacism, off-target gene editing) were examined.*